Image Segmentation and Adaptive Contrast Enhancement for Haze Removal

Bao Zhu

A Thesis

in

The Department

of

Electrical and Computer Engineering

Presented in Partial Fulfillment of the Requirements

for the Degree of

Master of Applied Science (Electrical and Computer Engineering) at

Concordia University

Montréal, Québec, Canada

December 2021

CONCORDIA UNIVERSITY

School of Graduate Studies

This is to certify that the thesis prepared

By: Bao Zhu

Entitled: **Image Segmentation and Adaptive Contrast Enhancement for Haze Removal**

and submitted in partial fulfillment of the requirements for the degree of

Master of Applied Science (Electrical and Computer Engineering)

complies with the regulations of this University and meets the accepted standards with respect to originality and quality.

Signed by the Final Examining Committee:

_____ Chair
Dr. M.O. Ahmad

_____ External Examiner
Dr. C.-Y. Su (MIAE)

_____ Examiner
Dr. M.O. Ahmad

_____ Supervisor
Dr. Chunyan Wang

Approved by _____
Dr. Yousef R. Shayan, Chair
Department of Electrical and Computer Engineering

_____ 2021

_____
Dr. Mourad Debbabi, Dean
Gina Cody School of Engineering and Computer Science

Abstract

Image Segmentation and Adaptive Contrast Enhancement for Haze Removal

Bao Zhu

Nowadays, hazing scenes are very frequent in images acquired outdoors. For such images to be used as input images of autonomous systems, it is important to restore the image details so that they can provide sufficient information to the system. As hazy images feature poor contrast due to degraded image variations, one can use a contrast enhancement method, such as CLAHE, to restore the image details. However, in case of very heavily hazy images, the image signal quality is severely degraded. Applying a strong enhancement may help to recover the details but will meanwhile generate very visible noise, affecting the image quality. In order to handle the problem of the conflict of the degree of enhancement and noise created in the process, it is thus necessary to develop a good algorithm with different enhancement based on a specific mask and signal variations in different regions.

In this thesis, a novel dehazing algorithm is proposed, which aims at heavily hazy images. In order to restore effectively image details that are almost invisible in hazy images without over enhancement in other foreground areas, the proposed algorithm involves a new adaptive CLAHE process, in which a stronger enhancement is applied to the areas of weaker variations, different from an existing version of improved CLAHE with adaptive clip limit. This new CLAHE is applied only to the foreground areas, by means of a protective mask, so that there will not be noise enhancement in the atmospheric background and the other flat areas. Each input image is segmented into foreground and background areas to generate the mask. In case of heavily hazy images, the gradient amplitudes of the signals and the noise are in the same level and it is thus very difficult to distinguish foreground and background areas. A new gradient matrix has been defined and a gradient feature vector proposed to detect the locally dominant gray level variations, with a view to identifying the pixels of very weak variations in foreground areas with the noise

presence. This gradient vector helps to distinguish the foreground and background areas in heavily hazy images, and the segmentation can be done effectively, which makes it possible to apply the new adaptive CLAHE without noise enhancement.

The proposed algorithm has been tested with different kinds of hazy images. In case of heavily hazy image input, it performs better, in terms of image detail restoration, than existing methods based on dark-channel-prior (DCP) or other form of CLAHE. It is effective with hazy images of high dynamic range. It is also useful in case of lightly hazy images.

Acknowledgments

At first, I would like to express my deep gratitude to my supervisor Dr. Chunyan Wang for her immense support and brilliant guidance during my study in Concordia University. I want to thank her for helping me to shape the ideas of this work. Her knowledge and expertise in the field enriches me a lot. I feel extremely privileged to be able to work under her supervision.

And also I want to thank my friends for the help and advice during my research. Their patience and kindness bring me a happy life.

Finally, I would like to thank my family for their love and supports. They always believes in me and give me the strength to successfully finish this work.

Contents

List of Figures

List of Tables

List of Acronyms and Abbreviations

HE	Histogram Equalization
AHE	Adaptive Histogram Equalization
CLAHE	Contrast Limit Adaptive Histogram Equalization
HDR	High Dynamic Range
LP	Low-pass
HP	High-pass
DCP	Dark Channel Prior
MSE	Mean Squared Error
PSNR	Peak Signal to Noise Ratio

List of Symbols

$I(i,j)$	Input image.
$I_g(i,j)$	Gray-scale of the input image.
$E(i,j)$	Gray-scale enhanced image .
$\mu_{(k,l)}$	Average value of the (k,l) window .
$\sigma_{(k,l)}$	Standard deviation value of the (k,l) window
$\mu(i,j)$	Average gray level of the neighborhood centered at (i,j) and sized $(2n+1)^2$ pixels.
$\sigma(i,j)$	Standard deviation of the neighborhood centered at (i,j) and sized $(2n+1)^2$ pixels.
$G(i,j)$	Gradient matrix generated by Sobel high pass kernels.
$G_\Sigma(i,j)$	Sum of $(2n+1)^2$neighborhood in each pixel position (i,j) of the $G(i,j)$.
$G_M(i,j)$	Maximum value of all elements in the $G_\Sigma(i,j)$.

Chapter 1

Introduction

1.1 Research topic and challenges

The quality of outdoor images can be severely degraded due to smog, dust, and other environmental or climactic issues. As the environment problems get worse, smog/haze gets thicker and appears more frequent. Outdoor images became hazier. Haze-removal became important part in processing images of outdoor scenes, and its results can make significant difference in the quality of the succeeding processing.

From image signal point of view, images of hazy scenes have very poor contrast. Image dehazing is, in fact, restoring the signal contrast to reveal original image details. One may use contrast enhancement methods, such as Contrast-Limited Adaptive Histogram Equalization (CLAHE)[1], to solve the problem. However, in an image of heavily hazy scene, as an example shown in Figure 1.1(a), the signal variations in some areas are hardly visible, due to the gradient degradation. Applying a strong contrast enhancement to such an image may help to restore some image details, but it can also amplify the image data fluctuations in flat areas, generating very visible noise, as shown in Figure 1.1(b).

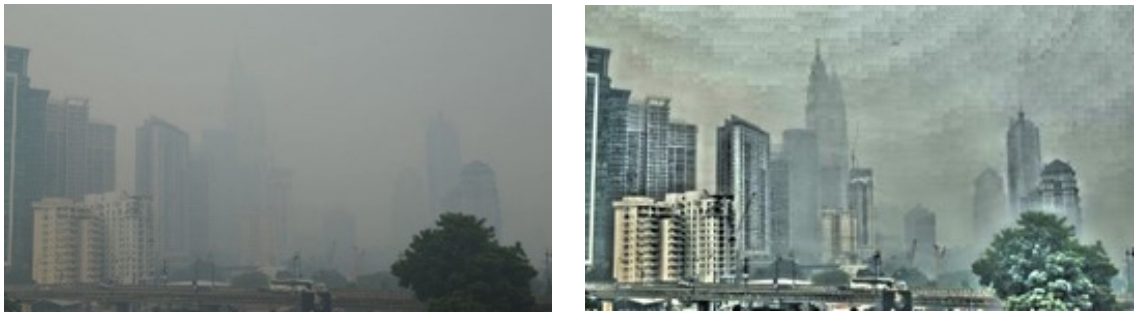

(a) (b)

Figure 1.1: (a) Original image. (b) Dehazed image by the CLAHE.

There are some dehazing methods reported. A good number of dark-channel-prior (DCP) methods[2][3][4] are developed based on an atmospheric scattering model[5]. They may be used to solve some image dehazing problems, but not effective in case of heavily hazy images, in which the gradient degradation is not uniform and very bad in some areas. Some of these methods allow users to adjust the strength of dehazing, i.e., in fact, the strength of contrast enhancement. However, similar to the case of applying adaptive histogram equalization for image dehazing, a DCP method can hardly lead to a good dehazing performance, in terms of image detail restoration, without creating visible noises in the output images.

1.2 Motivations and objective

The outdoor images are more and more frequently applied to various automatic control systems, for example, in traffic management and autopilot. Image processing modules, e.g., for object detection, in such systems are critical components for the performance. Lack of signal details in hazy input images could lead to a poor detection and failure of the systems. Hence, it is important to recover the signals before the processing for detection. A dehazing method, effective in the aspect of contrast enhancement for signal variations, is needed.

The objective of the work presented in this thesis is to develop an effective dehazing algorithm. It aims at heavily hazed outdoor images. The emphasis is on restoring severely degraded image details while minimizing the noise enhancement in flat areas. It can be used for dehazing purpose, or for image preprocessing in various detection systems.

1.3 Scope and organization

To achieve the objective, the algorithm is to be designed to perform a specific contrast enhancement, as a main problem in hazy images is poor contrast. One needs to enhance selectively the local image contrast, i.e., applying a stronger enhancement to the edge areas where signal variations degraded more due to thicker haze, while weak or no enhancement to the flat areas. To this end, it is important to identify edge areas and flat areas and the task will be difficult considering that the amplitudes of signal variations in some edge areas are not greater than the gray level fluctuations in flat areas. Hence, a method distinguishing signal gradients from noise gradients should be developed to identify low-gradient edge areas. Other image processing components, such as high-pass and low-pass filters will also be used in the new algorithm.

This thesis is organized as follows. In chapter 2, the fundamentals of image processing related to this work are described. Some of the existing methods for the haze removal relevant to the work are also presented.

Chapter 2

Background and Relevant Work

2.1 Introduction

Hazy images are of low quality due to the low contrast. If they are applied to systems of computer vision, the performance of these systems may be degraded. Therefore, dehazing is an important part in images pre-processing.

A dehazing process can be seen as a contrast enhancement. Various histogram equalization methods can be employed for dehazing purpose. Other approaches, such as those based on atmospheric models, are also reported for haze removal. Basic filtering operations are used in different dehazing processes. However, to achieve a good dehazing performance, particularly in case of heavily hazy images where signal details are severely damaged, adaptive filtering and contrast enhancement processes are needed.

In this chapter, some image processing fundamentals related to the proposed algorithm are presented in Subchapter 2.2. Examples of existing work relevant to haze removal are described in Subchapter 2.3.

2.2 Fundamentals related to the proposed method

2.2.1 Low-pass filters

The low pass filter is used to retain the low frequency information within an image while reducing the high frequency information. Many kinds of low-pass filters are employed to remove

high spatial frequency noise in digital image processing, such as mean filter, Gaussian filter, median filter and bilateral filter. Among these filters, the first two are commonly used because of their relatively low computation intensity and good performance.

Mean filtering is to smooth the image by replacing each pixel value with the mean of its neighbors. Like other filtering operations by convolution, its bandwidth is related to the kernels. A general mean value filter centered on (i, j) pixel position is defined as

$$g(i,j) = \frac{1}{m \times n} \sum_{s=-a}^{a} \sum_{t=-b}^{b} f(i+s, j+t)$$

where $m \times n$ is the total number of pixels in the neighborhood and $a = (m-1)/2$, $b = (n-1)/2$. The size of the neighborhood $m \times n$ determines the filtering bandwidth[6].

Another commonly used low-pass filter is Gaussian filter. It smooths the image by replacing the center pixel with the weighted average of the neighboring pixels. A 2-dimensional Gaussian function is defined as

$$g(x,y) = \frac{1}{2\pi\delta^2} e^{-\frac{x^2+y^2}{2\delta^2}}$$

The 2 Gaussian characteristics are presented in Figure 2.1, with 2 different δ values. The Gaussian function is used to determine the filtering kernel. The bandwidth of the filter is determined by the parameter δ and/or the neighborhood size. A larger δ implies a smaller bandwidth of Gaussian filter and greater smoothing.

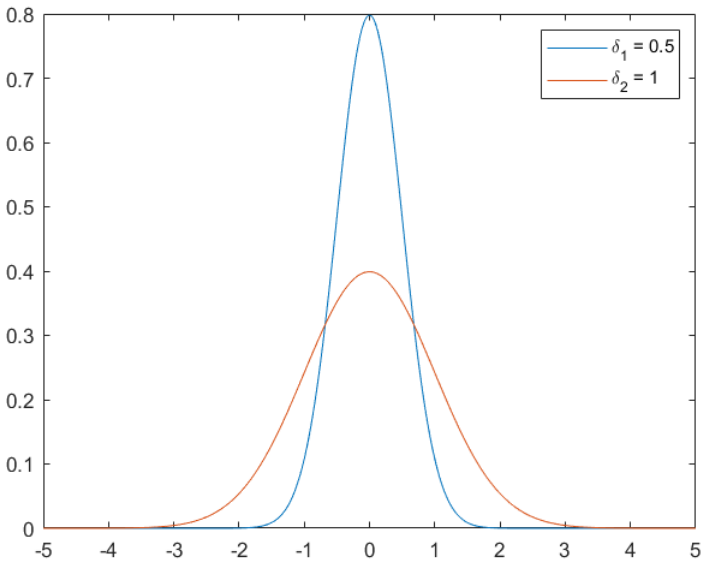

Figure 2.1: Gaussian characteristics with $\delta_1 = 0.5$ and $\delta_2 = 1$.

where δ_1 is smaller than δ_2. One can adjust the value of δ to achieve a compromise between excessive blur of the desired image features and excessive undesired variation in the smoothed image due to noise and fine texture.

In many image processing applications, low-pass filters with variable bandwidths. Hence there are adaptive filters, in which bandwidths are not fixed, but adapting to the local signal variations. One such example is guided filter[7], and its filter coefficients are related to the local variance and its covariance with another image. In the work presented in this thesis, both basic low-pass and adaptive low-pass filters are used, which is presented in Chapter 3.

2.2.2 High-pass filters

The high-pass (HP) filters tend to pass signals with a frequency higher than a certain cut-off frequency and attenuates signals with frequency lower than the cut-off frequency. In image processing, the high-pass filters are often used to detect the edge signals in the image. HP filters with Sobel and Laplacian kernels are frequently used to detect various gray level variations.

Sobel kernels are commonly used in high-pass filters. The 4 kernels shown in Figure 2.2 are used to detect the gray level variation in the horizontal, vertical and diagonal directions, respectively.

-1	0	1
-2	0	2
-1	0	1

(a) 0^o

0	1	2
-1	0	1
-2	-1	0

(b) 45^o

1	2	1
0	0	0
-1	-2	-1

(c) 90^o

2	1	0
1	0	-1
0	-1	-2

(d) 135^o

Figure 2.2: Four Sobel kernels.

Laplacian HP filters are also commonly used to detect gray level variations. Figure 2.3 illustrate 3 frequently used Laplacian kernels. The kernel shown in Figure 2.3(a) is used to detect the data variation in the neighborhood of 3×3 pixels, without specifying the directions, whereas those shown in Figure 2.3(b) and (c) are used to detect 2 different orthogonal directions, respectively.

-1	-1	-1
-1	8	-1
-1	-1	-1

(a)

0	-1	0
-1	4	-1
0	-1	0

(b)

-1	0	-1
0	4	0
-1	0	-1

(c)

Figure 2.3: Three Laplacian kernels.

2.2.3 Histogram Equalization

Histogram equalization is used in different applications of image processing for contrast enhancement because of its simplicity and effectiveness. The standard histogram equalization (HE)[8][9] is to enhance the contrast of an image by using the cumulative distribution function (CDF) of the gray level distribution of the image. The gray level transfer function of standard HE can be expressed as

$$h(x) = round\left(\frac{cdf(x) - cdf_{min}}{(M \times N) - cdf_{min}} \times 255\right)$$

where $cdf(x)$ is the cumulative distribution function of the image gray level signals, $0 \leq x < 256$, cdf_{min} is the minimum non-zero value of $cdf(x)$, $M \times N$ is the number of the pixels of the image.

Through such a transformation process, the intensities can be distributed on the histogram using the full range of intensity. However, if the input image already has a high dynamic range, the effect of a standard HE will be weakened.

This limitation in standard HE can be overcome by adaptive histogram equalization (AHE)[10]. In this method, the image is divided into a number of tiles and the histograms for each tile are generated to create an individual transfer function for each local HE. However, AHE has a tendency

to overamplify noise in relatively homogeneous regions of an image. In such regions, most local pixels have very similar gray levels, which form a high peak in the local histogram. This high peak then leads to the transformation functions are mapped from a narrow range of pixel values to the whole range of the result image. Eventually, small variations in a relatively flat region are amplified and this region becomes a less flat region with noise[11].

In order to avoid such a drawback of AHE, an adaptive method was presented, which is known as contrast limited adaptive histogram equalization (CLAHE). Differing from AHE method, CLAHE limits the local contrast enhancement by clipping the bins in the histogram that are higher than a global limit before computing the CDF. Therefore, one can reduce the slope and hence alleviate the gray level stretching around those peaks. In most applications, CLAHE has proven to be successful for the enhancement of low-contrast images. However, a global clipping value has limitation on the variation in one image, the contrast is increased, noise also increase specially in homogeneous regions.

2.3 Relevant work

2.3.1 Image haze removal based on contrast enhancement

In this thesis work, the input image often has a low contrast due to the presence of haze in the atmosphere. The standard image dehazing problem can be viewed as a type of image contrast enhancement. As a classical method, histogram equalization (HE) performs an easy and effective way in contrast enhancement. To overcome the shortage of the standard HE methods, many variations fall into making the transformation function of HE more adaptive to local image signals. It can be done by modulating the cumulative functions in local tile[12] or using the weighted threshold in HE[13].

In some other advanced AHE methods, the parameters involved in the mapping function is modulated according to its homogeneity, for example CLAHE. However, in the standard CLAHE, all tiles will be applied by a unique clip limit value may results the histogram clipping improperly in some regions. In order to reduce the artifacts introduced by the standard CLAHE methods, [14]illustrates a new tone mapping algorithm, each neighbor tile is applied with an individual clip

limit defined as

$$\alpha = a \times mean\left(I_{k,l}\left(i,j\right)\right) + 12\left(1-a\right) \times var\left(I_{k,l}\left(i,j\right)\right)$$

where α is the normalized clip limit, a is a weight factor between [0,1], $I_{k,l}\left(i,j\right)$ is the pixel gray level on i^{th} row and j^{th} column and factor 12 is used to renormalize the variance value.

According to the method presented above, one can see that the image will be enhanced more where the regions have a larger variance value. in other words, a low contrast region will not be enhanced much for avoiding the noise generation in flat area, e.g. The sky region. Therefore, the algorithm has a limitation on heavily hazed image enhancement.

So far, the majority of the dehazing methods try to faithfully invert the standard hazy image degradation model. However, the parameters used in many methods are often hard to estimate accurately. In[15], the standard haze model is obtained in the HSV color space for contrast enhancement due to its robustness to color distortion. The advantage of this new approach is enhancing the image contrast through the inaccurately estimated parameters with intentional bias. During to base on the HSV color space, it still has limitation on the kinds of image with heavily hazed images, which have hardly color signals in them.

In[16][17], in order to estimates the transmission map to maximize the contrast of the output image. In this method develop a cost function to measure the contrast, which combines the standard deviation term and the histogram uniformness term.

2.3.2 Image haze removal based on degradation model

In almost every practical scenario the light reflected from a surface is scattered in the atmosphere before it reaches the camera. This is due to the presence of aerosols such as dust, mist, and fumes which deflect light from its original course of propagation[18]. In long distance photography or foggy scenes, the process has a substantial effect on the image in which contrasts are reduced and surface colors become faint[19]. Such degraded photographs often lack visual vividness and appeal, and moreover, they offer a poor visibility of the scene contents.

Light passing through a scattering medium is attenuated along its original course and is distributed to other directions. This process is commonly modeled mathematically by assuming

that along short distances there is a linear relation between the fraction of light deflected and the distance traveled[20]. More formally, along infinitesimally short distances $d\mathbf{r}$ the fraction of light absorbed is given by $\beta \times d\mathbf{r}$ where β is the medium extinction coefficient due to light scattering. Integrating this process along a ray emerging from the viewer, in the case of a spatially varying β , gives

$$t = exp\left(-\int_0^d \beta\left(\mathbf{r}\left(s\right)\right) ds\right)$$

where $\mathbf{r}$ is an arc-length parametrization of the ray. The fraction t is called the transmission and expresses the relative portion of light that managed to survive the entire path between the observer and a surface point in the scene, at $\mathbf{r}(d)$, without being scattered[21]. In the absence of black-body radiation the process of light scattering conserves energy, meaning that the fraction of light scattered from any particular direction is replaced by the same fraction of light scattered from all other directions. The equation that expresses this conservation law is known as the Radiative Transport Equation[22].Assuming that this added light is dominated by light that underwent multiple scattering events, allows us to approximate it as being both isotropic and uniform in space. This constant light, known as the airlight[23] or also as the veiling light, can be used to approximate the true in-scattering term in the full radiative transport equation to achieve the following simpler image formation model[24][25][26]

$$I\left(X\right) = t\left(X\right) J\left(X\right) + \left(1 - t\left(X\right)\right) A$$

where this equation is defined on the three RGB color channels. $I(X)$ stands for the observed image, A is the airlight color vector, $J(X)$ is the surface radiance vector at the intersection point of the scene and the real-world ray corresponding to the pixel $X = (x, y)$, and $t(X)$ is the transmission along that ray[19]. This degradation model is commonly used to describe the image formation in the presence of haze[27][28][29][30]. The goal of haze removal is recover $J(X)$, A and $t(X)$ from $I(X)$. The scene transmission $t(X)$ is distance-dependent:

$$t(X) = e^{-\beta d(X)}$$

where β is the attenuation coefficient of the atmosphere and $d(x)$ is the distance of the scene at pixel

X. Generally, β is wavelength dependent and therefore $t(X)$ is different per color channel[25][29]. This dependency has been assumed negligible in previous single image dehazing methods to reduce the number of unknowns. The transmission $t(X)$ acts as a matting coefficient between the scene $J(X)$ and the airlight A[3].

In[19], a new method for recovering a haze-free image is proposed. The algorithm, according to the paper, interprets the image through a model that accounts for surface shading in addition to the scene transmission. Based on this refined image formation model, the image is broken into regions of a constant albedo and the airlight-albedo ambiguity is resolved by deriving an additional constraint that requires the surface shading and medium transmission functions to be locally statistically uncorrelated. This method is passive; it does not require multiple images of the scene, any light-blocking based polarization, any form of scene depth information, or any specialized sensors or hardware. This approach is physically sound. However, it cannot handle heavily hazy images well and may fail in the cases where the assumption is broken.

Some other methods of atmospheric model are based on the statistics of outdoor haze-free images[2]. It is based on an observation that in most of the local regions which do not cover the sky, some pixels (called dark pixels) very often have very low intensity in at least one color (RGB) channel. In hazy images, the intensity of these dark pixels in that channel is mainly contributed by the airlight. These dark pixels can provide an estimation of the haze transmission to restore the haze-free image. However, the dark channel prior has limited effects when the scene object is inherently similar to the airlight over a large local region and no shadow is cast on it.

2.4 Summary

In this chapter, basic image filtering elements for image dehazing are presented. Also, as the dehazing problem is in fact a contrast enhancement problem, various histogram equalization methods are described. Adaptive histogram, like CLAHE, can be effective in many dehazing operations. But for heavily hazed images, there is a problem of conflict, i.e., revealing sufficient image details versus minimizing the noise creation. There are also dehazing methods, based on an atmospheric model, for dehazing, and they have similar problems of image-details against image noises.

To solve the problem mentioned above, in the following chapter, a haze removal algorithm, based on the image segmentation and adaptive contrast enhancement are proposed. The segmentation is to separate the foreground areas from the background so that different methods can be applied, without conflict of image detail enhancement and noise generation. Both segmentation and enhancement are challenge tasks in case of heavily hazed images. New methods are developed to secure the effectiveness of the proposed haze removal algorithm.

Chapter 3

Haze Removal by Using Image Segmentation and Adaptive Contrast Enhancement

3.1 Overview

The objective of the work presented in this thesis is to develop an algorithm to restore heavily hazed outdoor images. It involves an effective image segmentation and a new version of CLAHE with adaptive clip limit, with a view to applying a strong contrast enhancement without generating visible image noise. A new gradient matrix is proposed to detect very weak signal variations with the presence of noise gradients of similar magnitudes.

As mentioned previously, the proposed algorithm aims at a good restoration of heavily hazy outdoor images. The key point in it is to make the contrast enhancement local-signal-dependent: The weaker the signal variations due to thicker haze, the stronger the enhancement to reveal more image details. However, this enhancement approach may cause a noise amplification in flat areas, such as part of sky in outdoor images. Hence, this algorithm comprises a stage of segmentation to identify the areas of objects and the areas of background, and a CLAHE-based enhancement method is proposed and applied only to the areas of objects. The block diagram of the processing is shown in Figure 3.1. The details of the processing are presented in the following subsections.

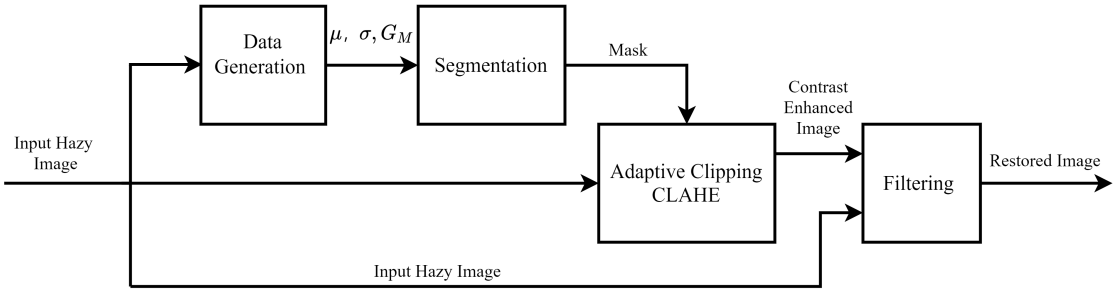

Figure 3.1: Block diagram of the proposed algorithm for haze removal.

3.2 Design of The Segmentation Processes

This work aims at segmenting the input image into background and foreground areas. The background is specifically atmospheric, i.e., air space, and all the other parts in the input image, such as buildings, trees or vehicles, belong to the foreground. Thus, the foreground comprises areas of more signals, and the gray level variations will be significantly enhanced, whereas the areas of atmospheric background is expected to receive a very modest enhancement to avoid noise amplification.

Gradient-based image segmentation has been used in haze removal operations[32][33]. In a normal case, as the foreground has more significant gray level variations, with respect to the flat background, simple gray level gradients can be used to differentiate foreground segments from the background ones. However, in images of severely hazy outdoor scenes, as the examples shown in Figure 3.2, the gray level variations of distant buildings are in the same level as that of the noise in the background. Thus, one needs to find other kinds of feature data to distinguish the foreground from the background.

(a) (b)

Figure 3.2: Examples of heavily hazed outdoor images.

To differentiate the signal gradients and noise ones, we propose to use 3 kinds of image data at each pixel position. The first two are $\mu(i,j)$ and $\sigma(i,j)$ of the original input image, representing data statistics in the neighborhood centered at pixel position (i,j). The third one is the gradient matrix, $G_\Sigma(i,j)$, it is specifically proposed for this image segmentation and produced from basic gradients. Let us use the following example to explain how the elements of this matrix are calculated in 2 steps.

In the first step, let us consider, in this example, the signal gradients in the 4 directions, i.e. $0^o, 45^o, 90^o$ and 135^o. The 4 Sobel kernels, as shown in Figure 3.3, are used to generate these gradient components. By doing so, 4 gradient components, $G(i,j) = [g_{0^o}, g_{45^o}, g_{90^o}, g_{135^o}]_{i,j}$, are produced at each pixel position. In other words, the 4 gradient maps are produced from each input image channel.

-1	0	1
-2	0	2
-1	0	1

(a) 0^o

0	1	2
-1	0	1
-2	-1	0

(b) 45^o

1	2	1
0	0	0
-1	-2	-1

(c) 90^o

2	1	0
1	0	-1
0	-1	-2

(d) 135^o

Figure 3.3: Sobel kernels used to detect the gray level variations in the 4 directions.

It should be noted that the gradient components have signed values. For example, if a component has a negative value in the direction of 45^o, it indicates the direction of gray-scale variations is $45^o + 180^o$.

In the second step, in each of the 4 gradient maps, the algebraic sum of the gradient components in a neighborhood of $(2n+1)^2$ pixels are calculated at each pixel position (i,j) to generate $G_\Sigma(i,j)$. As shown in Figure 3.4, 4 gradient sum maps are generated from the 4 gradient maps, respectively. Therefore, at each pixel position (i,j), there is a matrix of gradient-sums, $G_\Sigma(i,j) = [g_{\Sigma 0^o}, g_{\Sigma 45^o}, g_{\Sigma 90^o}, g_{\Sigma 135^o}]_{i,j}$. For example, $g_{\Sigma 45^o}(i,j)$ is the algebraic sum of the $(2n+1)^2$ signed values of the gradient components in the direction of 45^o. Hence, each element in $G_\Sigma(i,j)$ represents the gradient components of the neighborhood in a specified direction, and the algebraic summation of the signed gradient values helps to eliminate some gradient components produced by noise.

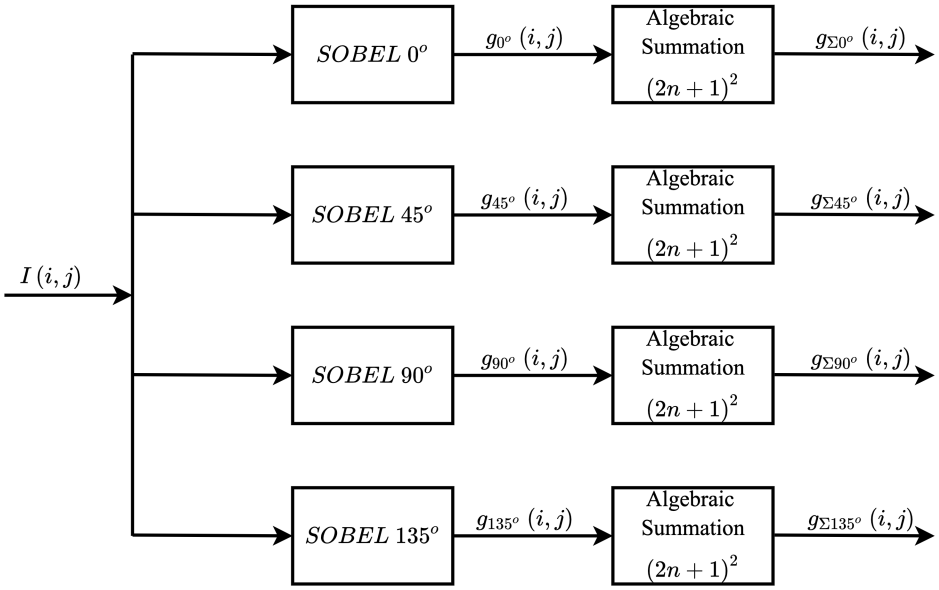

Figure 3.4: Procedure to generate 4-elemen $G_\Sigma(i,j) = [g_{\Sigma 0^o}, g_{\Sigma 45^o}, g_{\Sigma 90^o}, g_{\Sigma 135^o}]$.

In case of gray-scale input image, at each pixel position (i,j), $G_\Sigma(i,j) = [g_{\Sigma 1}, g_{\Sigma 2}, g_{\Sigma 3}, g_{\Sigma 4}]$. In case of color image of RGB channels, there will be 4 gradient maps, from each of the RGB color maps. In other words, at each pixel position, there is a matrix of 3×4 elements, expressed as follows.

$$G_{\Sigma RGB}(i,j) = \begin{bmatrix} g_{\Sigma R1} & g_{\Sigma R2} & g_{\Sigma R3} & g_{\Sigma R4} \\ g_{\Sigma G1} & g_{\Sigma G2} & g_{\Sigma G3} & g_{\Sigma G4} \\ g_{\Sigma B1} & g_{\Sigma B2} & g_{\Sigma B3} & g_{\Sigma B4} \end{bmatrix}_{i,j}$$

From the matrix $G_\Sigma(i,j)$, the gradient feature value $G_M(i,j)$ is generated. It is the maximum value of the elements of $G_\Sigma(i,j)$, if the input is a gray-scale image. If the input image consists of color RGB channels, the feature value $G_M(i,j)$ can be defined in different ways. We propose the following three options.

- Option 1: $G_M(i,j)$ is the maximum magnitude of all the elements in $G_\Sigma(i,j)$.
- Option 2: $G_M(i,j)$ is the arithmetical or algebraic sum, depending on processing requirement, of the elements in the column where the element of the maximum magnitude in the matrix is found. For example, in the matrix $G_{\Sigma\ RGB}(i,j)$ shown above, if the maximum magnitude is found in the second column, $G_M(i,j) = |g_{\Sigma R2} + g_{\Sigma G2} + g_{\Sigma B2}|$, or $G_M(i,j) = |g_{\Sigma R2}| + |g_{\Sigma G2}| + |g_{\Sigma B2}|$.

- Option 3: Instead of a simple summation of the three elements in Option 2, in Option 3, $G_M(i,j)$ is the square root of the sum of their squared values. In the example given above, it is expressed as $G_M(i,j) = \sqrt{{g_{\Sigma R2}}^2 + {g_{\Sigma G2}}^2 + {g_{\Sigma B2}}^2}$.

In general, one can use K high pass kernels to generate the gradient maps in K directions from each image channel. Then, the K elements of $G_\Sigma(i,j)$ are calculated based on the gradients in the neighborhoods of $(2n+1)^2$ pixels in these gradient maps. The neighborhood size is determined according to image features to be detected. The $G_M(i,j)$ is based on the maximum value of the elements in $G_\Sigma(i,j)$, and it carries information of the dominant gray level variations in the neighborhood.

The set of data comprising $G_M(i,j)$, standard deviation and average value of the input image signal, represents the information of the gray level distribution and the dominant edge orientation in the neighborhood surrounding the pixel position (i,j). In the proposed algorithm, the data of the input image is processed to generate σ-map, μ-map, and G_M-map. These maps are then used to segment the input image into the regions of the foreground and those of the background.

The segmentation is a process of 2 steps as shown in Figure 3.5. Apparently, these two conditions in the segmentation process are independent. In order to correspond with the algorithm in this thesis, the Figure 3.5(a) are used for an explanation.

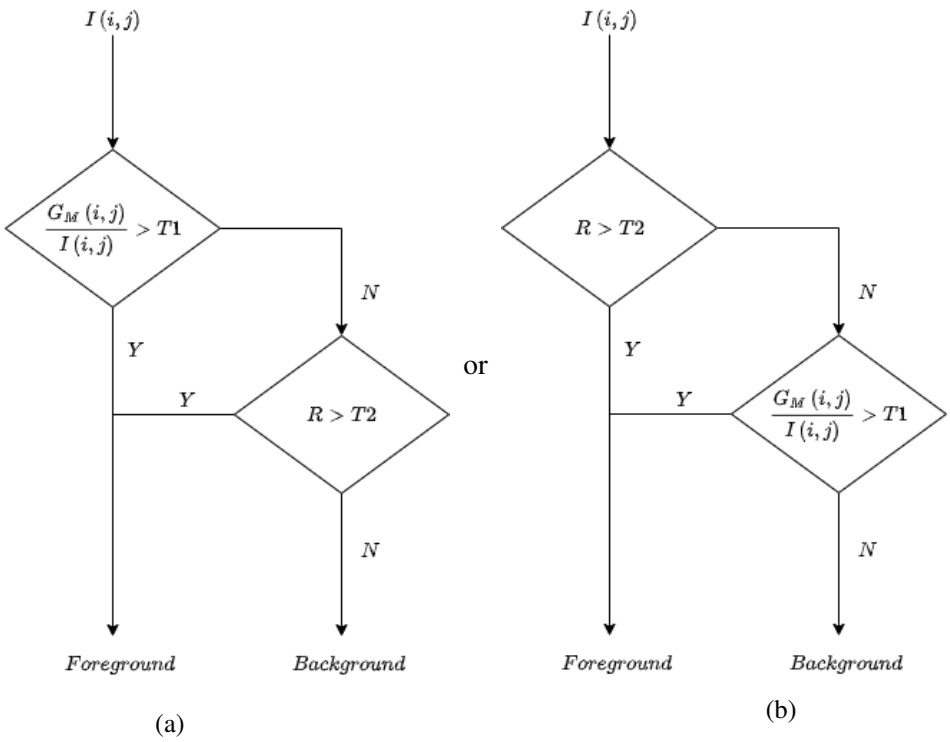

Figure 3.5: Segmentation process. $T1$ and $T2$ are pre-determined thresholds.

In the first step, $G_M(i,j)$ is normalized with the gray-scale $I(i,j)$. The pixels having higher values of the normalized $G_M(i,j)$ are considered as foreground pixels.

In the second step of the segmentation, the pixels not identified as foreground in the first step are examined. A pixel having a small value of $G_M(i,j)$ can be part of the foreground. For example, the pixels of smaller flat area, such as brighter parts in the buildings located in the very left-hand side of the image shown in Figure 3.2(b), should be indicated in the foreground. In this case, the gray-scale variations in a small neighborhood can be insignificant, however, those in a large neighborhood surrounding it can be significant. If $\sigma(i,j)$ is used to measure the variations in a neighborhood of $(2n+1)^2$ pixels, the $\sum_{k=-m}^{m}\sigma(i+k,j+k)$ can be used to measure the variations in the neighborhood of $[2(m+n)+1]^2$. Hence, in the second step, we use the following ratio

$$R = 10^{-2} \times \frac{\left[\sum_{k=-m}^{m}\sigma(i+k,j+k)-\sigma(i,j)\right]^8}{\mu^4(i,j)}$$

to identify the pixels having weak $G_M(i,j)$ but located in the foreground regions. As the significance of variations is related to their average gray-scale in the areas, they are normalized by $\mu(i,j)$. The ratio is made to be determined by the signals of the pixels in the neighborhood,

and $\sigma(i,j)$ is excluded from the calculation of the ratio. Pixels having higher values of the ratio are considered to belong to the foreground. The results of the segmentation are used to create binary masks, with '0' indicating the foreground and '1' is the background regions, respectively.

(a) (b)

Figure 3.6: (a) Binary image in which the black pixels have higher G_M values than white ones. (b) Binary mask generated by the stage of the segmentation.

The images shown in Figure 3.6 is produced by the segmentation in the 2 steps applied to the image shown in Figure 3.2(a). One can have the following observations.

- 1. The binary map shown in Figure 3.6(a) is produced by applying the first step with the normalized G_M. One can see that the outlines of very distant buildings are included in the foreground. It indicates that, by means of the gradient feature value G_M, the proposed segmentation method is effective in identifying the foreground pixels from the background even though their gray-scale variations are in a similar level.

- 2. The pixels of smaller flat areas are also included in the foreground, by means of the ratio R, with a view to a good enhancement in the following stage.

After the 2-setp segmentation, a very simple morphological operation is performed to remove small spots. The mask generated at the end of the segmentation is shown in Figure 3.6(b).

3.3 Adaptive Contrast Enhancement

As mentioned previously, a good contrast enhancement is a key issue in haze-removal operations. CLAHE is likely the best adaptive histogram equalization method for contrast enhancement, and its clip limit can be used to adjust the dose of the enhancement. Using the mask

generated in the image segmentation in Subchapter 3.1, one can apply a lightly dosed enhancement to the background areas without risk of noise enhancement. For the enhancement in the foreground areas, we propose an adaptive clipping CLAHE to make the contrast gain better adapt to the local signals.

As indicated in its name, CLAHE is to limit the contrast enhancement in flat areas, where gray-scale variations are very insignificant and the histogram has very high peaks, to avoid visible noise amplifications. It is done by clipping high peaks, which results in reduced transformation coefficients. In case of the haze-removal presented in this thesis, some foreground areas have very insignificant gray-scale variations, which is indicated by high concentration of gray-scale distributions. If the CLAHE method is applied in a conventional manner, the contrast enhancement in the foreground areas of poor contrast will be limited, leading to an unsatisfactory result. Therefore, we propose an adaptive clipping CLAHE, in which the clip-limit is determined based on the local variations. In the foreground areas, the smaller variations, indicated by smaller value of standard deviations in tiles, the stronger enhancement by means of less clipping.

If $(2m+1)^2$ is the number of pixels in each tile, $H_{avg} = (2m+1)^2/256$ represents the height of bins in a uniform distribution in the histogram, and H_{clip} is the maximum height of the bins after clipping, then $\alpha = H_{clip}/H_{avg}$, $\alpha > 1$. In the proposed adaptive clipping, α is determined by the standard deviation and average value of each tile. A larger α value results in less clipping in the histogram and a stronger enhancement. It is defined as

$$\alpha = 1 + 0.4\frac{\mu_t(k,l)}{\sigma_t(k,l)^{1.2}}$$

and the maximum height of the bins after clipping is

$$H_{clip} = \left(1 + 0.4\frac{\mu_t(k,l)}{\sigma_t(k,l)^{1.2}}\right)(2m+1)^2/256$$

where (k,l) is the coordinates of the tiles, $\mu_t(k,l)$ and $\sigma_t(k,l)$ are the average gray level and the standard deviation of $(k,l)^{th}$ tile. The clip limit is made to be inversely related to the variations measured by $\sigma_t(k,l)$. In the proposed haze-removal algorithm, the more signal degradation by thicker haze, the smaller signal variations, the higher clip limit, and the stronger enhancement.

It should be noted that the above-described adaptive clip-limit is different from that presented in [4]. In that algorithm, to avoid noise enhancement in flat areas, the clip-limit was made to decrease

the enhancement with the signal variance. The clip-limit in this work adapts to the local signal in the opposite direction, as there is no concern of noise enhancement in the flat background.

As mentioned previously, the input image can be a gray-scale or color image. If the input image I is composed of RGB maps, like the one shown in Figure 3.2(a), one can convert it to a gray-scale image I_g, and then apply the proposed enhancement to the gray-scale image. The image shown in Figure 3.7(a) is the contrast enhanced gray-scale image, produced by the proposed enhancement. Many image details that were veiled by haze in the original input appear in the enhanced image. However, one can also notice some noise, mostly due to the discontinuity between the foreground and the background areas. A filtering stage is designed to remove it.

3.4 Adaptive Filtering

Applying the adaptive CLAHE in segmented areas can result in the discontinuity in the contrast-enhanced image I_e. The filtering stage is designed to remove it. From I_e and I_g, the gray-scale image converted from the input image I, one can generate the transformation coefficient $E\left(i,j\right) = I_e\left(i,j\right)/I_g\left(i,j\right)$ at each pixel position to form the e-map. As shown in Figure 3.7, V_{I_g}, the variance of the signal from I_g, $V_{I_g,E}\left(i,j\right)$, the covariance of I_g and $\beta = V_{I_g,E}/V_{I_g}$, the ratio of covariance and variance, are calculated in a neighborhood of $\left(2r+1\right)^2$ pixels centered at $\left(i,j\right)$.

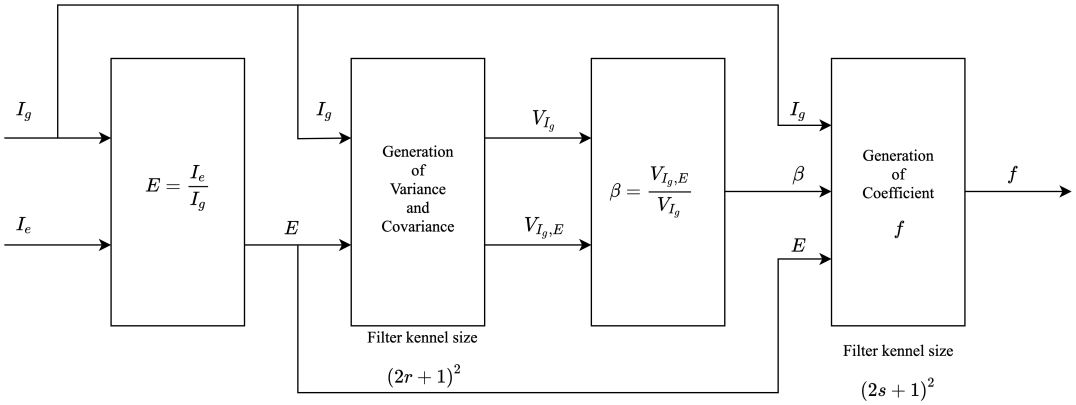

Figure 3.7: procedure to generate the filtering coefficient $f\left(i,j\right)$. The variance of I_g, the covariance of I_g and e are calculated in a neighborhood of $\left(2r+1\right)^2$ pixels. The average values of the ratio $\beta = V_{I_g,E}/V_{I_g}$ and e are calculated in a neighborhood of $\left(2s+1\right)^2$.

The filtering coefficient $f\left(i,j\right)$ is defined as follows:

$$f\left(i,j\right) = \mu_\beta\left(i,j\right) \times \left[I_g\left(i,j\right) - \mu_{I_g}\left(i,j\right)\right] + \mu_E\left(i,j\right)$$

where μ_{I_g}, μ_β and μ_E are the average values of I_g, β and E, respectively, in the window of $(2s+1)^2$ pixels.

This filtering is local signal-adaptive. In flat areas, $f(i,j) \approx \mu_E(i,j)$, and in the other areas, $f(i,j)$ is adjusted bi-directionally around $\mu_E(i,j)$ by $\mu_\beta(i,j) \times \left[I_g(i,j) - \mu_{I_g}(i,j)\right]$ to remove strong discontinuity while preserving the enhancement achieved by the adaptive CLAHE in I_e. The filtering coefficient $f(i,j)$ is applied to the input image to produce a new contrast-enhanced image. Figure 3.8(b) illustrates the filtered gray-scale image produced from the image shown in Figure 3.8(a). The quality of the image is evidently improved by this filtering.

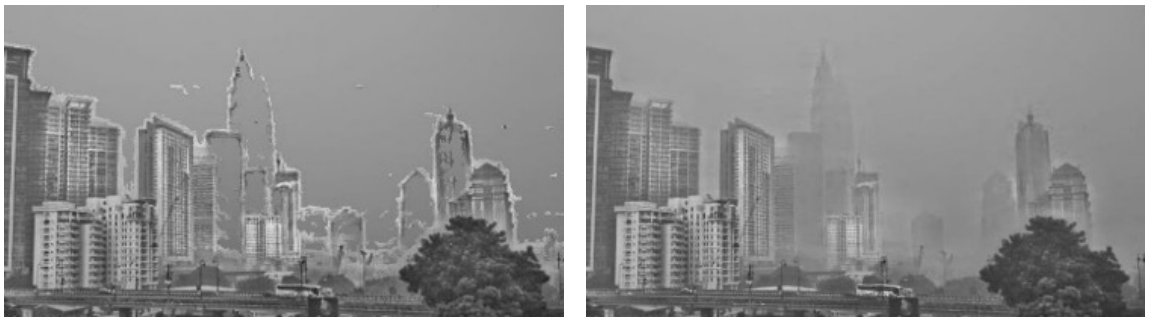

(a) (b)

Figure 3.8: (a) Contrast-enhanced image before the filtering. (b) Contrast-enhanced and filtered image.

3.5 Color Information and Color Restoration

In case of color hazy image, the color information is used, as described in Subchapter 3.2, to produce G_M that is used to generate the mask, and it is also used in the contrast enhancement. In the stage of the CLAHE-based enhancement, the local histogram is established with the pixels of all the 3 tiles from the 3 color maps, it is then clipped to generate the cumulative distribution function (CDF). This CDF is applied to the gray-scaled input image I_g, converted from the color input, to produce a gray-scale enhanced image I_e. The filtering coefficient map (f-map), produced based on the data of the I_g and I_e/I_g , is applied to each of the 3-original input RGB maps to produce a color image. If the original color input does not look “gray”, i.e., the color signal is not degraded to zero, the color restoration can be satisfactory.

3.6 Summary

In this thesis, an adaptive contrast enhancement algorithm has been proposed to restore signal details from heavily hazy images, where a good deal of signal variations in the foreground areas are degraded to the level of noise in flat area. The challenge in the design is to apply a strong enhancement to such signals without noise amplification. It has been achieved by three elements. Firstly, a specific gradient matrix is defined to generate a gradient feature value used to identify the pixels of very weak signals with the presence of noise of similar amplitude. Together with other signal data, the image is well segmented into the foreground and background areas. Then a CLAHE-based enhancement method is developed and applied in the foreground areas while the background is protected from noise enhancement. Finally, an effective filtering operation is performed to improve the visual quality of the restored image, while preserving the enhanced image details. The effectiveness of the proposed algorithms has been demonstrated by the test results. Though the algorithm is designed for haze removal, it can also be applied for other image quality enhancements.

In the next chapter, the simulations with different types of hazed image are described and the analysis of the results is presented for the evaluation of its effectiveness.

Chapter 4

Simulation Results and Evaluation

4.1 Introduction

The algorithm proposed in this thesis is to restore heavily hazed outdoor images. MATLAB simulations have been conducted to evaluate the effectiveness of the algorithms. In this chapter, the simulation processes and the evaluation results are presented.

Though the proposed algorithm mainly aims at the heavily hazed images, it has been tested with various types of hazy images. As mentioned previously, hazy images have poor contrast and the dehazing problem is in fact a contrast enhancement problem, while some attempted to solve it with various versions of Dark Channel Prior (DCP). The test results are compared with those resulting from the four algorithms, i.e., the CLAHE with adaptive clip-limit[14], Dark Channel Prior (DCP)[2], and 2 DCP-based algorithms[3][4].

The computation procedure of the proposed algorithm is illustrated in Figure 4.1. The qualitative results of the simulations with different kinds of images are presented in Subchapter 4.2. To test the algorithm with quantitative measures, synthetic hazy images of natural scenes have been created and the test results are presented in Subchapter 4.3.

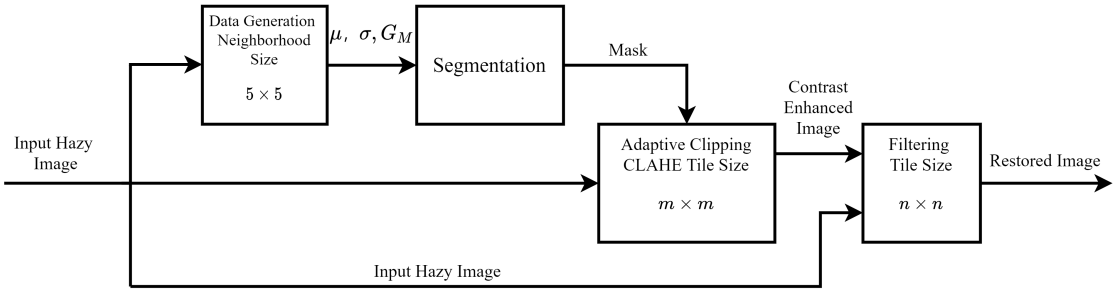

Figure 4.1: Block diagram of the proposed algorithm for haze removal. The neighborhood size to calculate the gradient vectors in Data Generation is 5×5. The tile size in CLAHE is m×m and the neighborhood size to calculate the statistical feature data in Filtering is n×n. Both m and n are specified in the Subchapters 4.2 and 4.3.

4.2 Qualitative Results

The qualitative tests are to assess the visual quality of the dehazed images resulting from the proposed algorithm. To test its effectiveness in different hazy/smog situations, three kinds of natural-scene images have been used, images of heavily hazed scenes, high-dynamic-range (HDR) images of medium-level haze, and images of low-level haze. The results of these 3 kinds are found in the following 2 sub-subchapters. The results presented in this subchapter have been generated with the tile size 25×25 in the stage of CLAHE and the neighborhood size 27×27 to calculate the statistical feature data in the block Filtering shown in Figure 4.1. As the dehazed images of these natural-scene images are not available, one cannot measure the dehazing performance quantitatively.

4.2.1 Simulation with images of heavily hazed scenes

The proposed algorithm is designed to enhance the contrast of heavily hazed images without adding visible noise. Four images of heavily hazed outdoor scenes are used in this part of the tests.

Figure 4.2(a) illustrates a typical scene covered by heavy haze, and details of distant buildings are hardly visible. The results generated by the 5 different algorithms, including the proposed one, are presented in Figures 4.2 (b) $\sim$ (f). One can see that CLAHE with adaptive clip-limit[14] provides a good contrast enhancement but also generates visible noise in flat areas, as shown in Figure 4.2(b). There is also perceivable noise in the dehazed image in Figure 4.2(c), given by Dark Channel Prior (DCP)[2]. The images shown in Figure 4.2(d) and (e) are given by 2 DCP-based algorithms[3][4],

and, though the colors of the images are more enhanced, the noise is more visible with respect to the others. In terms of restoration of severely degraded image details and noise avoidance, the proposed algorithm has evidently a better performance, as shown Figure 4.2(f), resulting from the proposed contrast enhancement that adapts to hazed scenes and applied under the effective protection of the mask.

(a) (b) (c) (d) (e) (f)

Figure 4.2: (a) Original image. (b) Dehazed image by the CLAHE with adaptive clip-limit[14]. (c) Dehazed image by the Dark Channel Prior (DCP)[2]. (d) Dehazed images by the DCP-based algorithms[3]. (e) Dehazed images by the DCP-based algorithms[4]. (f) Dehazed image by the proposed algorithm.

The images shown in Figures 4.3(a), 4.4(a), and 4.5(a) are also of heavily hazed scenes. By observing the results shown in Figure 4.3 $\sim$ 4.5, given by the 5 different algorithms, one can reach the same conclusion that the proposed algorithm gives the best dehazing performance, in terms of revealing the faded image details and minimizing the noise generation. Under the protection of the specifically generated masks, its special adaptive enhancement, i.e., more enhancement with lower contrast in the original input image, can effectively result in a better dehazing performance than the adaptive CLAHE and DCP-based algorithms.

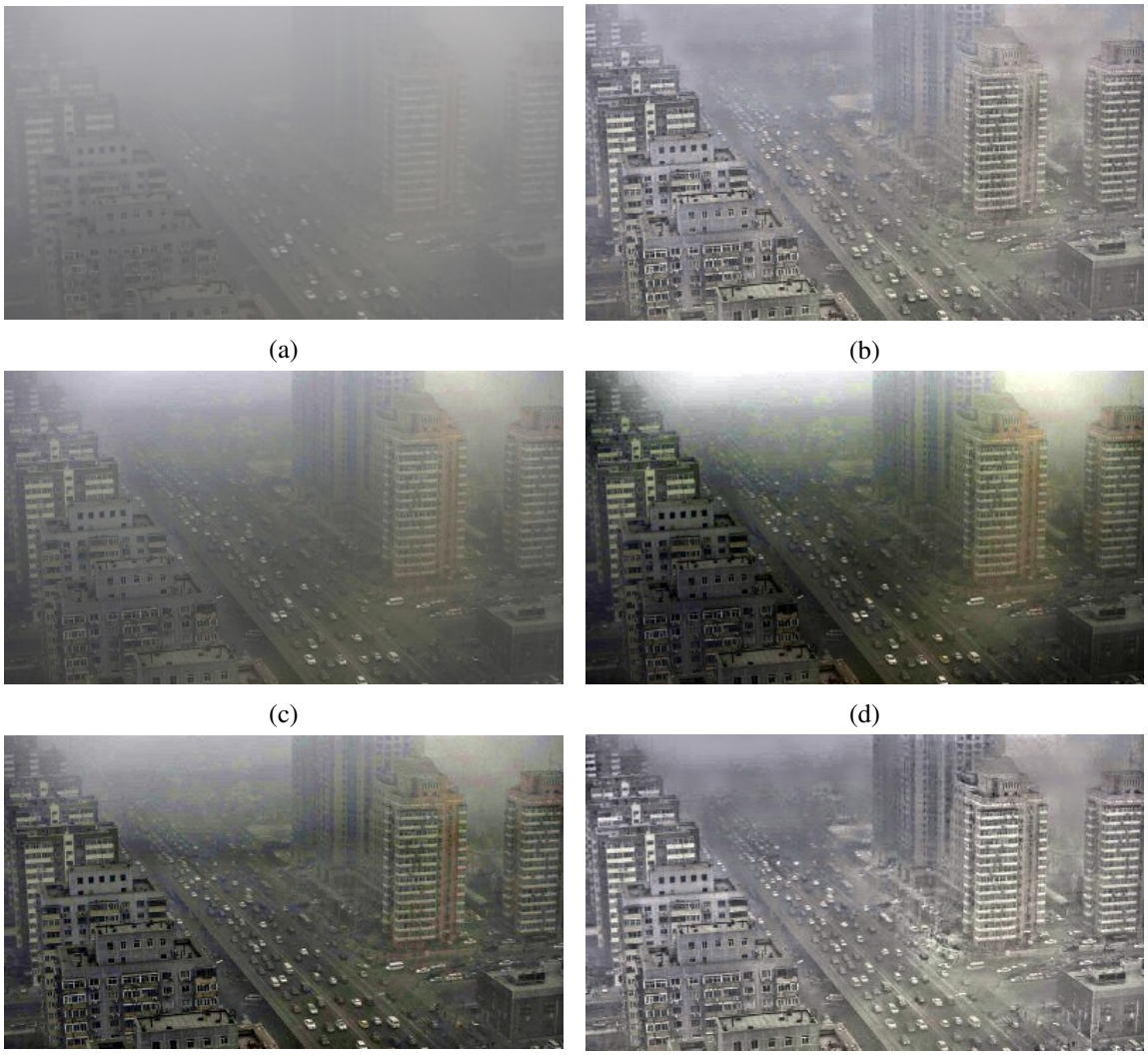

(a) (b) (c) (d) (e) (f)

Figure 4.3: (a) Original image. (b) Dehazed image by the CLAHE with adaptive clip-limit[14]. (c) Dehazed image by the Dark Channel Prior (DCP)[2]. (d) Dehazed images by the DCP-based algorithms[3]. (e) Dehazed images by the DCP-based algorithms[4]. (f) Dehazed image by the proposed algorithm.

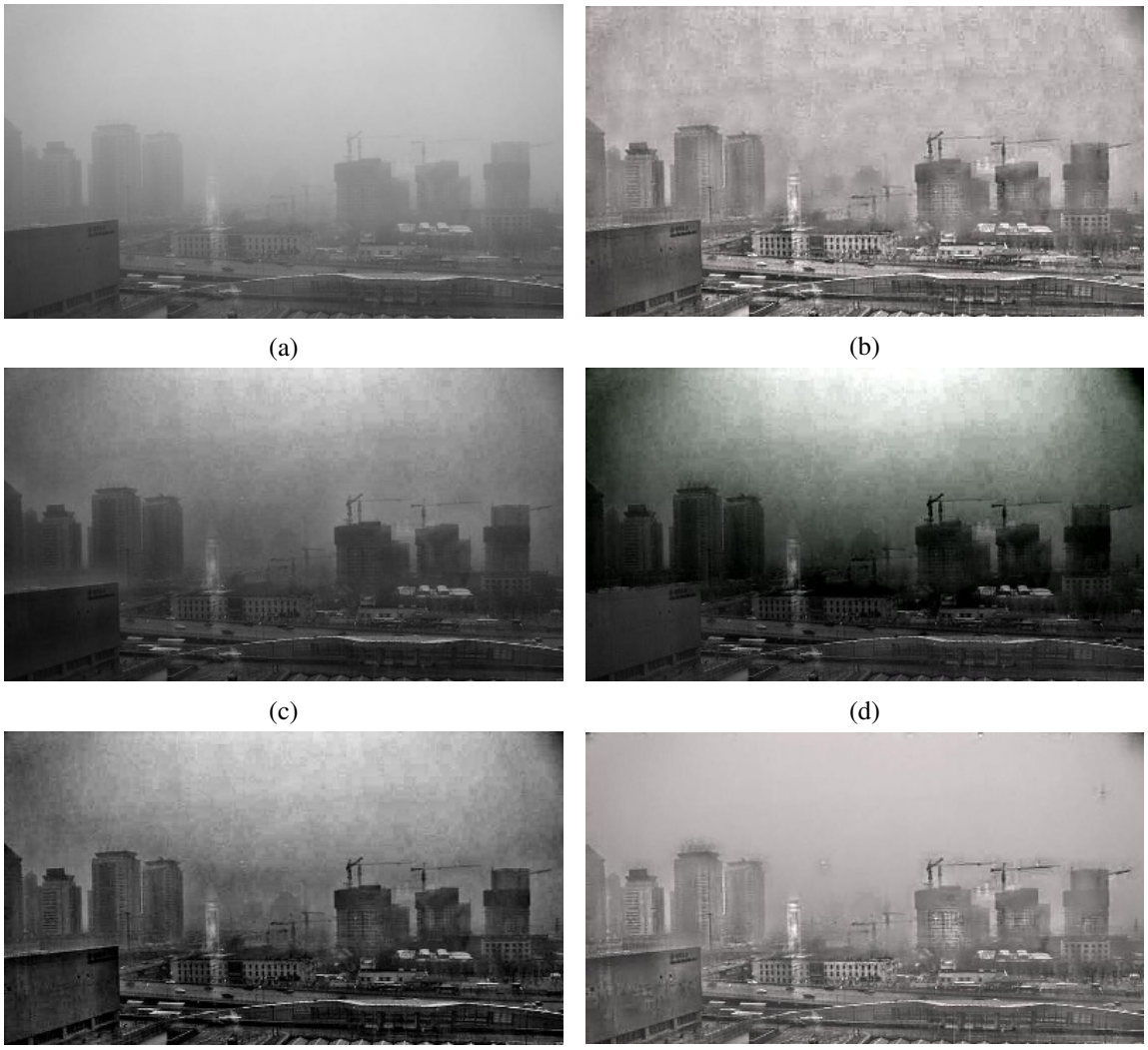

(a) (b) (c) (d) (e) (f)

Figure 4.4: (a) Original image. (b) Dehazed image by the CLAHE with adaptive clip-limit[14]. (c) Dehazed image by the Dark Channel Prior (DCP)[2]. (d) Dehazed images by the DCP-based algorithms[3]. (e) Dehazed images by the DCP-based algorithms[4]. (f) Dehazed image by the proposed algorithm.

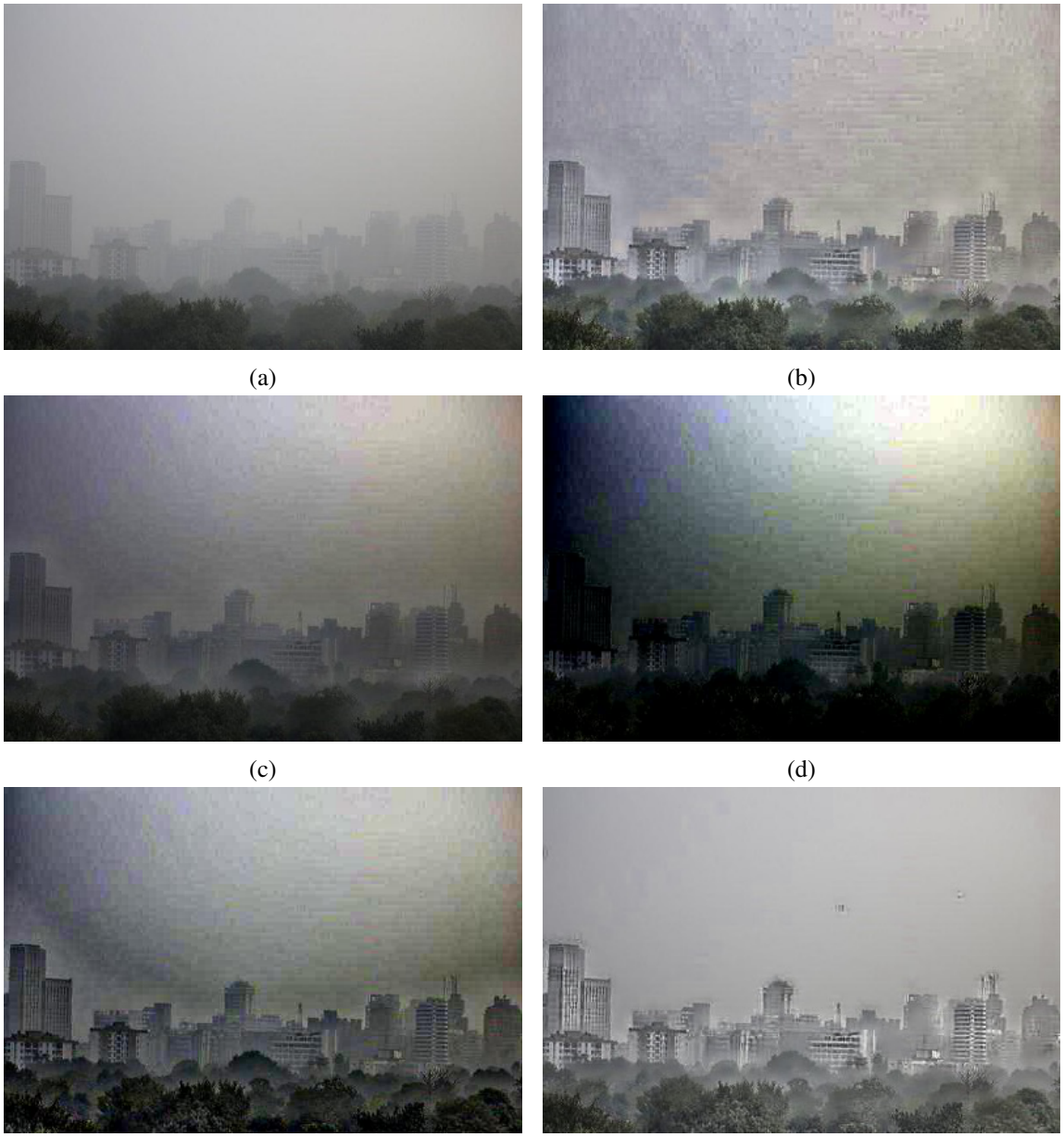

(a) (b) (c) (d) (e) (f)

Figure 4.5: (a) Original image. (b) Dehazed image by the CLAHE with adaptive clip-limit[14]. (c) Dehazed image by the Dark Channel Prior (DCP)[2]. (d) Dehazed images by the DCP-based algorithms[3]. (e) Dehazed images by the DCP-based algorithms[4]. (f) Dehazed image by the proposed algorithm.

4.2.2 Simulation with HDR images and other cases

The proposed algorithm has also been tested with hazy images of high dynamic range (HDR). Four images of this kind and their dehazed images are presented in this subchapter. As the intensity varies over a very wide range in each of these images, it is difficult to achieve a good dehazing performance over the entire range.

The image shown in Figure 4.6(a) is acquired from an HDR scene. To remove haze from such an image, the challenge is to enhance the contrast in all the regions of different intensity levels while minimizing noise enhancement. Comparing dehazed images shown Figure 4.6(b), (c), (d), (e) and (f), one can find that the 2 algorithms involving CLAHE, i.e., the proposed one and that with adaptive clip-limit[14], give the best overall enhancement. In case of the proposed algorithm, thanks to the protection mask, shown in Figure 4.6(f), the noise enhancement in the upper part of the dehazed image is not as pronounced as that in Figure 4.6(b). The 3 DCP algorithms[2][3][4] perform poorly in this case. In particular, it is difficult to use any of them to enhance the contrast in the lower section of the input image where the original intensity is low.

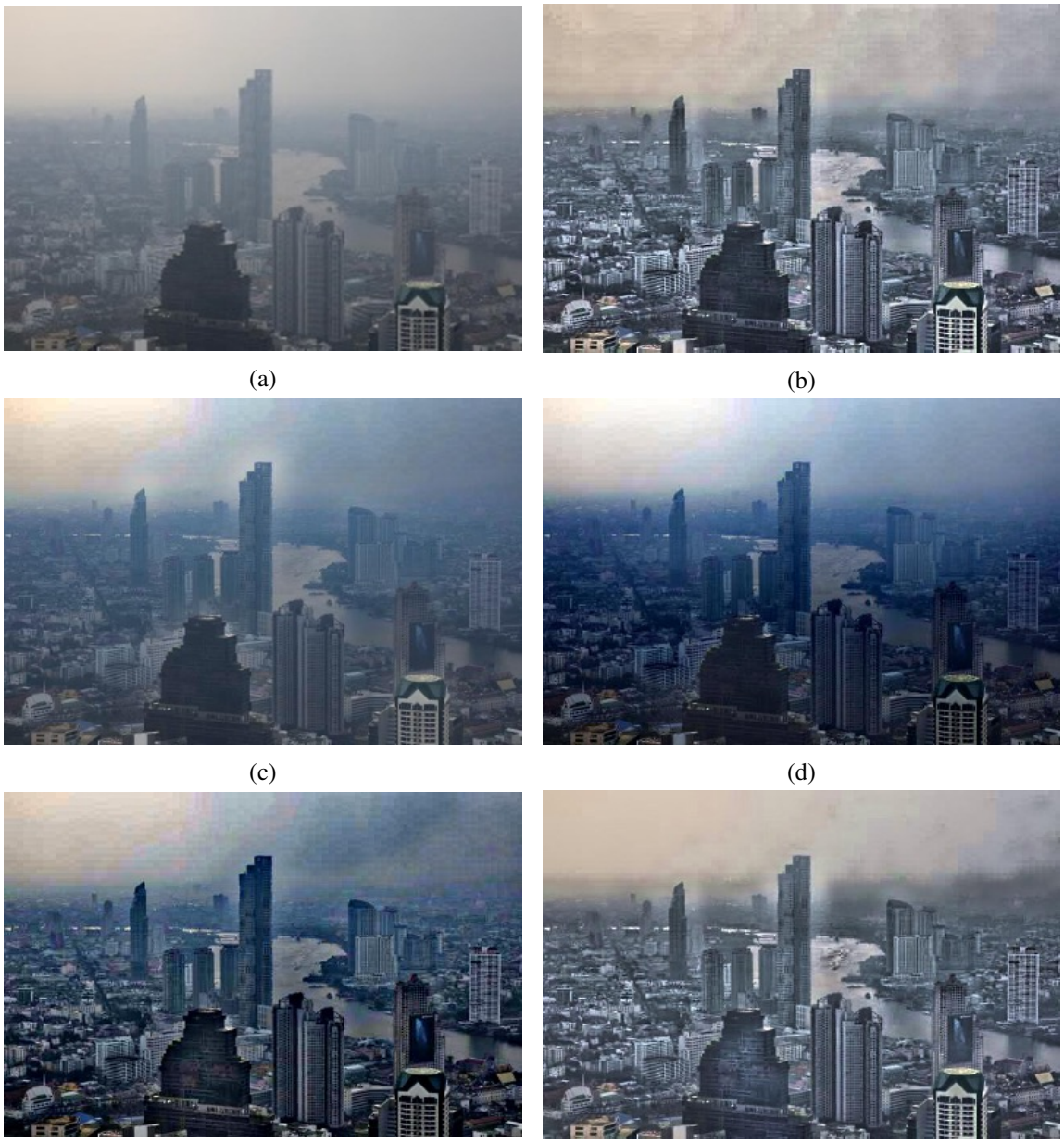

(a) (b) (c) (d) (e) (f)

Figure 4.6: (a) Original image. (b) Dehazed image by the CLAHE with adaptive clip-limit[14]. (c) Dehazed image by the Dark Channel Prior (DCP)[2]. (d) Dehazed images by the DCP-based algorithms[3]. (e) Dehazed images by the DCP-based algorithms[4]. (f) Dehazed image by the proposed algorithm.

The image shown in Figure 4.7(a) is also of HDR scene. Similar to the case shown in Figure 4.6, the algorithms involving CLAHE perform better than those of DCP. The weakness of the CLAHE with adaptive clip-limit is the noise enhancement in the flat areas, e.g., the top section of the image, whereas it is avoided in the proposed algorithm. One can observe similar performance comparison in the cases illustrated in Figure 4.8 and Figure 4.9 and reach the same conclusion.

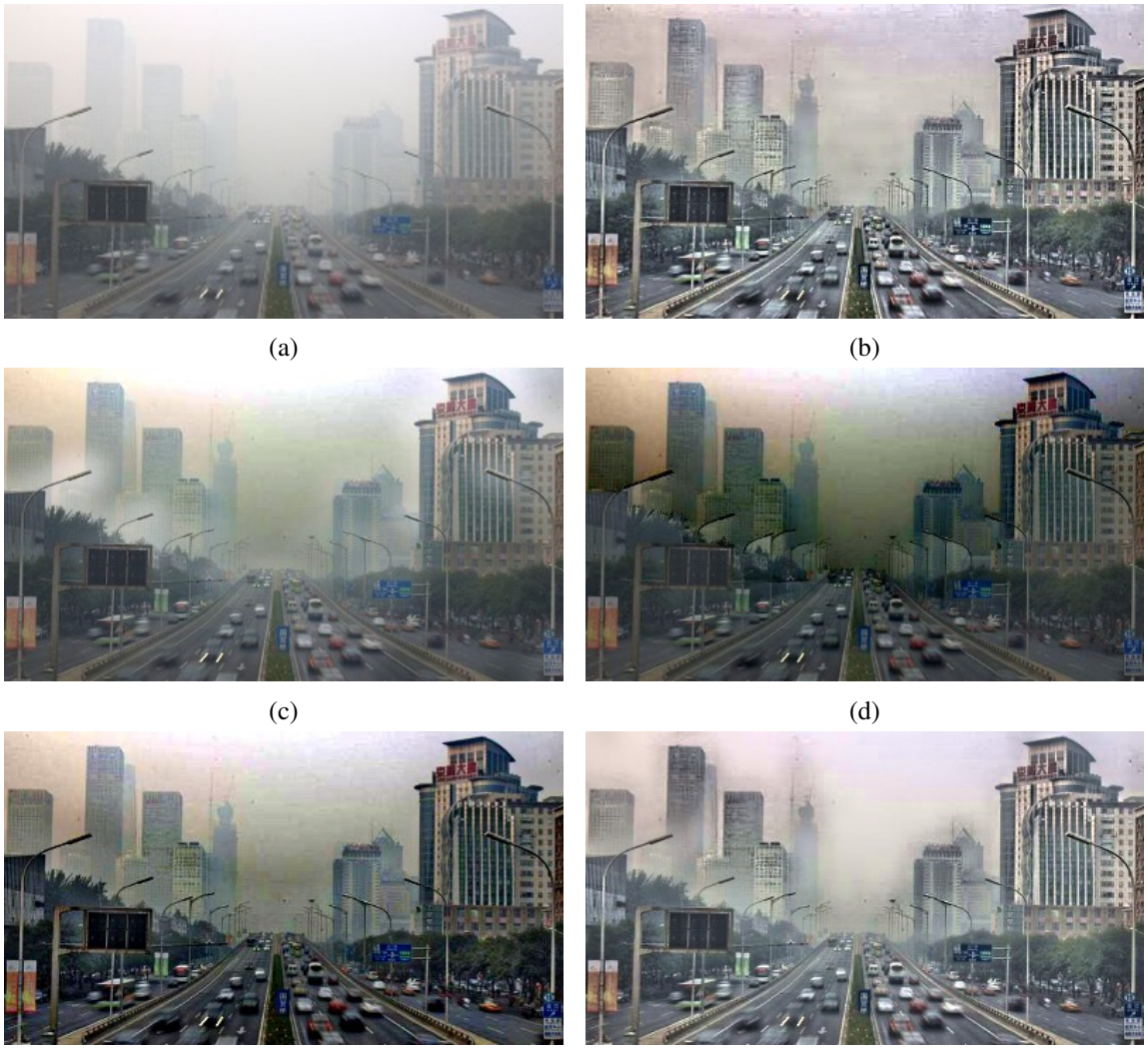

(a) (b) (c) (d) (e) (f)

Figure 4.7: (a) Original image. (b) Dehazed image by the CLAHE with adaptive clip-limit[14]. (c) Dehazed image by the Dark Channel Prior (DCP)[2]. (d) Dehazed images by the DCP-based algorithms[3]. (e) Dehazed images by the DCP-based algorithms[4]. (f) Dehazed image by the proposed algorithm.

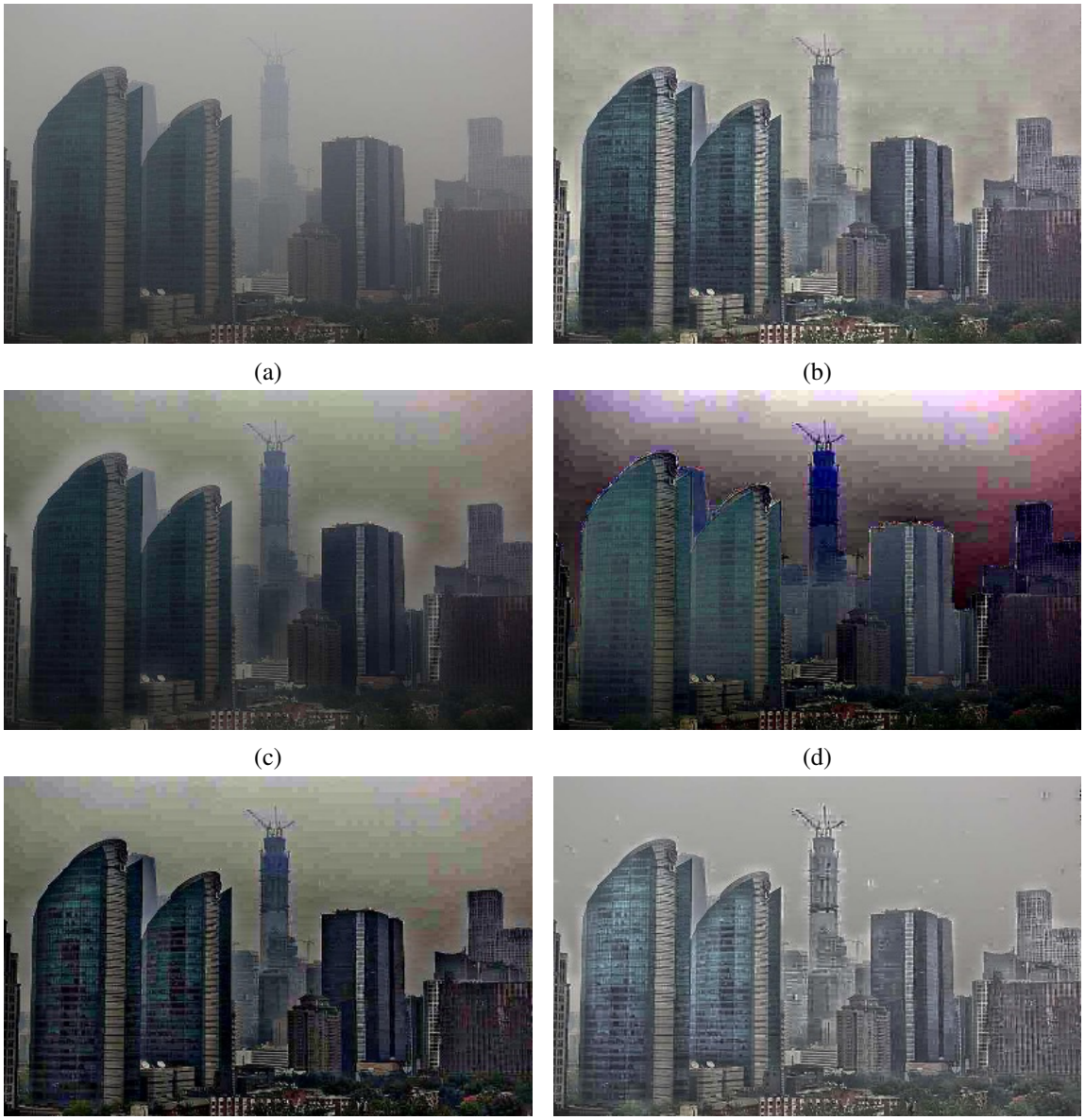

(a) (b) (c) (d) (e) (f)

Figure 4.8: (a) Original image. (b) Dehazed image by the CLAHE with adaptive clip-limit[14]. (c) Dehazed image by the Dark Channel Prior (DCP)[2]. (d) Dehazed images by the DCP-based algorithms[3]. (e) Dehazed images by the DCP-based algorithms[4]. (f) Dehazed image by the proposed algorithm.

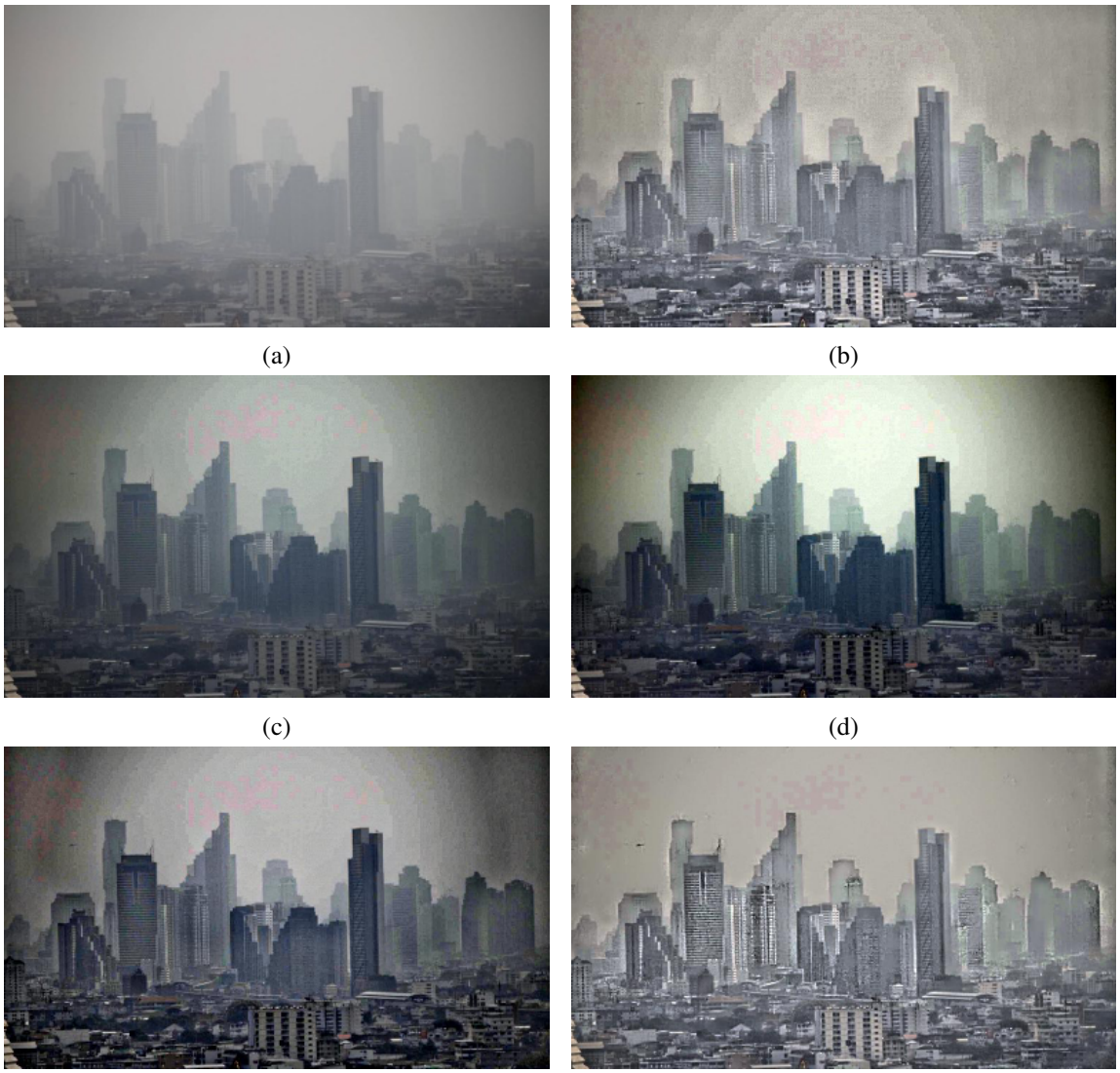

(a) (b) (c) (d) (e) (f)

Figure 4.9: (a) Original image. (b) Dehazed image by the CLAHE with adaptive clip-limit[14]. (c) Dehazed image by the Dark Channel Prior (DCP)[2]. (d) Dehazed images by the DCP-based algorithms[3]. (e) Dehazed images by the DCP-based algorithms[4]. (f) Dehazed image by the proposed algorithm.

Though the proposed algorithm is designed to remove heavy haze. It can also be used to process lightly hazed images as shown in Figure 4.10(a) and Figure 4.11(a), to recover image details. The dehazed images shown in Figure 4.10(f) and Figure 4.11(f) demonstrate that it is effectively useful in processing this kind of images.

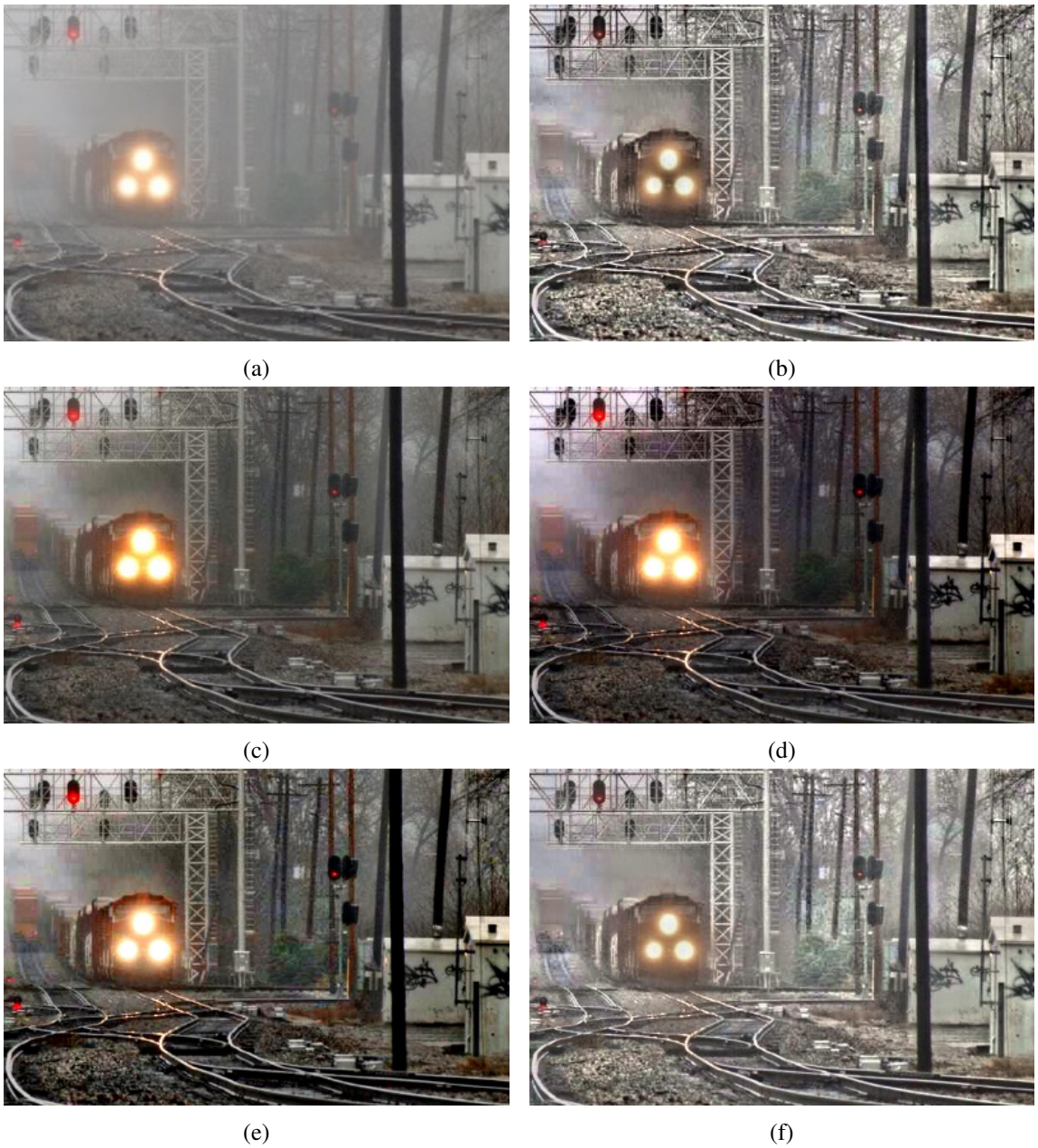

(a) (b) (c) (d) (e) (f)

Figure 4.10: (a) Original image. (b) Dehazed image by the CLAHE with adaptive clip-limit[14]. (c) Dehazed image by the Dark Channel Prior (DCP)[2]. (d) Dehazed images by the DCP-based algorithms[3]. (e) Dehazed images by the DCP-based algorithms[4]. (f) Dehazed image by the proposed algorithm.

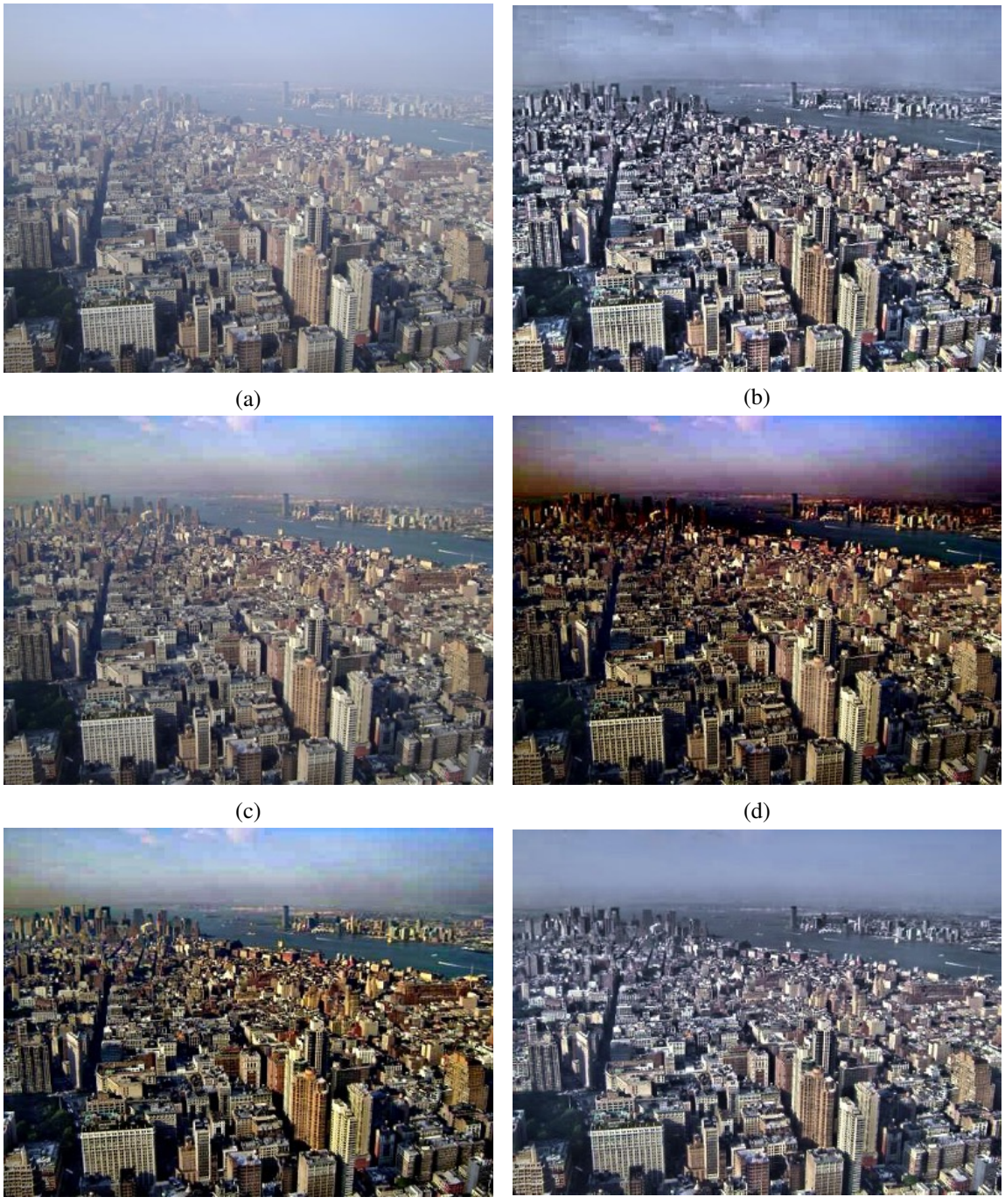

(a) (b) (c) (d) (e) (f)

Figure 4.11: (a) Original image. (b) Dehazed image by the CLAHE with adaptive clip-limit[14]. (c) Dehazed image by the Dark Channel Prior (DCP)[2]. (d) Dehazed images by the DCP-based algorithms[3]. (e) Dehazed images by the DCP-based algorithms[4]. (f) Dehazed image by the proposed algorithm.

4.3 Quantitative Results

In order to have quantitative measures, we applied an image manipulation tool to the clear-air outdoor images, illustrated in Figure 4.12(a), (c) and (e), to create the hazy images of the same scene, shown in Figure 4.12(b), (d) and (f). The tool allows to blur gradually in one direction, as if "white smog" were added to the image. The proposed algorithm is applied to the created image to generate a dehazed image. It is then compared to the reference, i.e., the original clear-air outdoor image to have objective results.

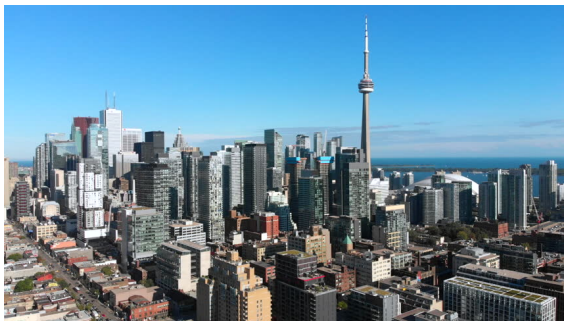

(a) Image 1

(b) Synthetically hazed image by Image 1

(c) Image 2

(d) Synthetically hazed image by Image 2

(e) Image 3

(f) Synthetically hazed image by Image 3

Figure 4.12: Examples of the clear-air outdoor images and the artificially created "hazy" images.

It should be mentioned that the artificially created hazy scenes are somehow different from the natural ones. As there is not much flexibility in adding "haze" to images, one cannot create various hazy scenes. The image quality of a dehazed image, produced by applying the proposed algorithm to a "hazy" image, is measure by peak signal to noise ratio (PSNR). It is defined as

$$PSNR = 20.log_{10}\left(\frac{I_{max}}{\sqrt{MSE}}\right)$$

$$MSE = \frac{1}{mn}\sum_{i=0}^{m-1}\sum_{j=0}^{n-1}\left[I\left(i,j\right) - I_e\left(i,j\right)\right]^2$$

where I_e is the dehazed image and I is the reference image, and I_{max} is the maximum pixel value in I_e.

The results presented in this subchapter have been obtained with 3 pairs of images, and the 3-original clear-air images are referred to as Image 1, Image 2, and Image 3. The PSNR values of the dehazed images are presented in Table 4.1, in comparison with those produced by the adaptive CLAHE[14] method and three other dehazing methods[2][3][4]. In each of these cases, the PSNR values resulted from these algorithms are in the same level. The dehazed images are presented in Figure 4.13 $\sim$ 4.15.

Input Image / Methods	Image1	Image2	Image3
Synthetically hazed image	11.1928	10.1712	11.7454
Boschetti *et al.* [14]	13.7047	12.1183	14.9193
He *et al.* [2].	14.2501	12.1779	16.1467
Berman *et al.* [3].	12.7756	12.2036	**16.4985**
Cho *et al.* [4].	14.3058	12.2197	16.2772
Proposed algorithm.	**14.392**	**12.2597**	16.3309

Table 4.1: PSNR values of the 3 dehazed images.

Figure 4.13 illustrates the hazed image produced by Image 1 and the 5 dehazed images by the 5 different algorithms, including the proposed one. One can see that the added haze covers, almost completely, the image details in the upper section. For example, the upper part of CN tour is made invisible. In the dehazed images illustrated in Figure 4.13(c) and (e), this part is also missing, whereas it appears in Figure 4.13(b), (d) and (f), produced by the algorithm[14],[3] and the proposed one, respectively. Comparing the images in Figure 4.13(b), (d) and (f), one can find that the dehazed

image resulted from the proposed algorithm has more image details, in particular in dark areas, and less noise in flat areas, whereas the other algorithm results in better colors.

The hazy images shown in Figure 4.14(a) and Figure 4.15(a) are similar to that in Figure 4.13(a), i.e., image details almost missing in the upper part. Also, similar to the case shown in Figure 4.13, the proposed algorithm produces more details, minimizing noise amplification in flat areas, and the other methods, all based on DCP, give better color results but may miss some details or produce visible noises.

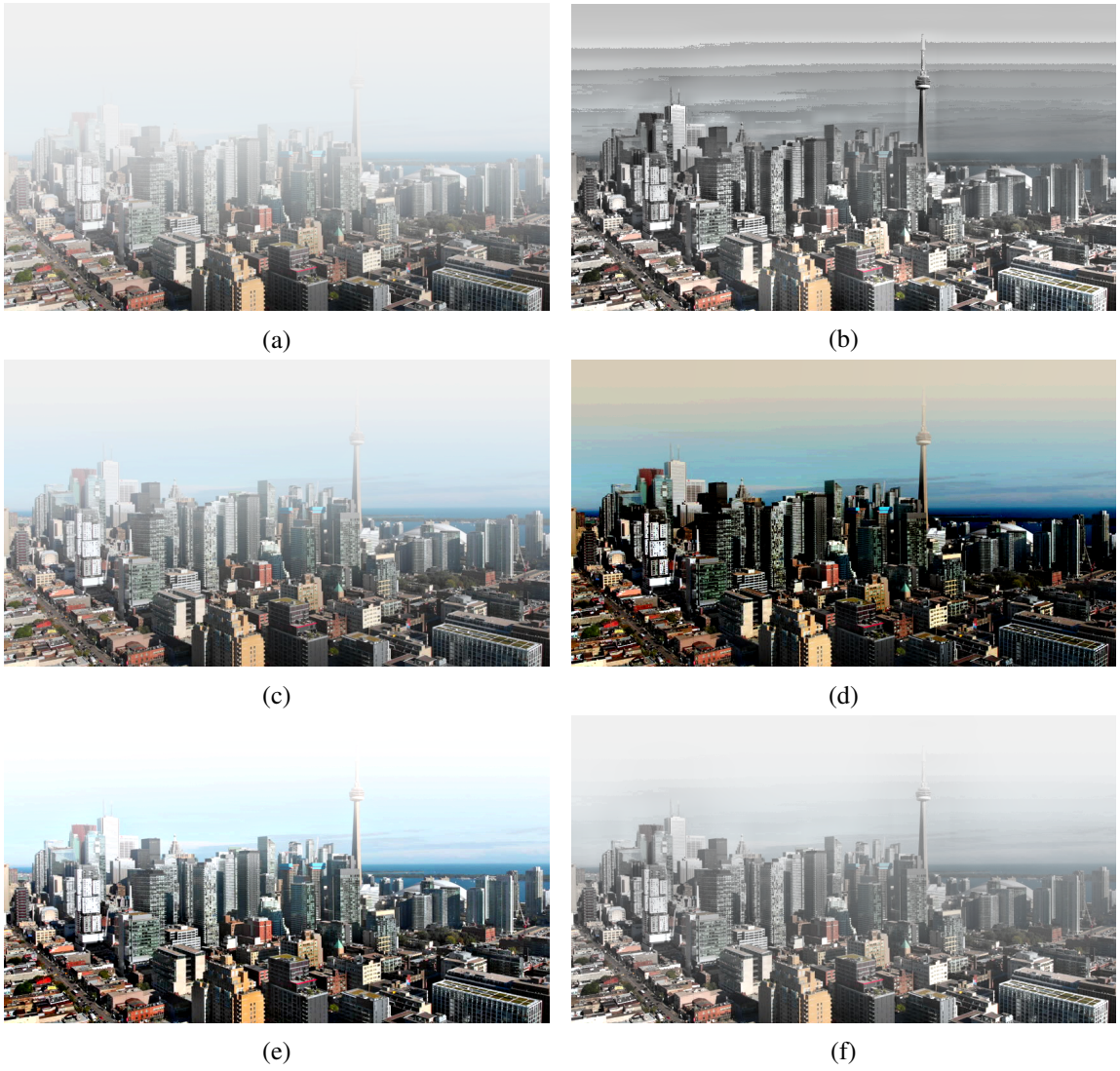

(a) (b) (c) (d) (e) (f)

Figure 4.13: (a) Synthetically hazed image by Image 1. (b) Dehazed image by adaptive CLAHE[14]. (c) Dehazed image by Dark Channel Prior (DCP)[2]. (d) Dehazed images by DCP-based algorithms[3]. (e) Dehazed images by DCP-based algorithms[4]. (f) Dehazed image by proposed algorithm.

(a) (b) (c) (d) (e) (f)

Figure 4.14: (a) Synthetically hazed image by Image 2. (b) Dehazed image by adaptive CLAHE[14]. (c) Dehazed image by Dark Channel Prior (DCP)[2]. (d) Dehazed images by DCP-based algorithms[3]. (e) Dehazed images by DCP-based algorithms[4]. (f) Dehazed image by proposed algorithm.

(a) (b) (c) (d) (e) (f)

Figure 4.15: (a) Synthetically hazed image by Image 3. (b) Dehazed image by adaptive CLAHE[14]. (c) Dehazed image by Dark Channel Prior (DCP)[2]. (d) Dehazed images by DCP-based algorithms[3]. (e) Dehazed images by DCP-based algorithms[4]. (f) Dehazed image by proposed algorithm.

4.4 Summary

This chapter is dedicated to the presentation of the simulation results of the proposed algorithm to evaluate its performance in haze removal. It has been demonstrated that the proposed algorithm is very effective to restore image details in heavily hazy images, without creating visible noise in flat areas. Also, it gives better performance, with respect to DCP-based algorithms, in case of HDR images. In case of images of low-level haze, the proposed algorithm can be used to enhance the image signal. The simulation results also show that the proposed algorithm does not have advantage in color enhancement, compared with the DCP-based algorithms, and more work is needed in this aspect.

Chapter 5

Conclusion

Hazing scenes are nowadays very frequent in images acquired outdoors. For such images to be used as input images of autonomous systems, such as object detections for autopilot, it is very important to restore image details so that they can provide the systems with sufficient information so that the system can operate correctly.

In general, hazy images feature poor contrast due to degraded image variations. One can use a contrast enhancement method, such as CLAHE, to restore the image details. However, in case of very heavily hazy images, the image signal quality is severely degraded. Applying a strong enhancement may help to recover the details but will meanwhile generate very visible noise, affecting the image quality.

In this thesis, a novel dehazing algorithm has been proposed, aiming at applications to heavily hazy images. Many image details in such cases are hardly visible. In order to effectively restore them without over enhancement in other areas, the proposed algorithm involves a new adaptive CLAHE process. It is designed to apply a stronger enhancement to the areas of weaker variations, differing itself from existing CLAHE of adaptive clip limit. This new CLAHE is applied only to the foreground areas, by means of a protective mask, so that there will not be noise enhancement in the atmospheric background and the other flat areas. To generate the mask, each input image is segmented into foreground and background areas. In case of heavily hazy images, the gradient amplitudes of the signals and the noise can be in the same level and it is thus very difficult to distinguish foreground and background areas. A new gradient matrix has been defined and a gradient feature vector proposed to detect the locally dominant gray level variations, with a view

to identifying the pixels of very weak variations in foreground areas with the noise presence. This gradient vector helps to distinguish the foreground and background areas in heavily hazy images, and the segmentation can be done effectively, which makes it possible to apply the new adaptive CLAHE without noise enhancement.

The proposed algorithm has been tested with different kinds of hazy images. In case of heavily hazy image input, it performs better, in terms of image detail restoration, than existing methods based on DCP or other form of CLAHE. It is effective with hazy images of high dynamic range. It is also useful in case of lightly hazy images.

There are a few avenues for the future work in this subject domain of image dehazing. One of them is the color restoration. Besides intensity signal variations, the color components in hazy images can also be degraded. The color restoration in low or mid-level hazy images can easily done by means of histogram equalization, as the color signal loss due to haze is not serious. A heavily hazy image looks light-gray, as the 3 color components are more or less equalized. Color restoration in such images is, no doubt, a challenge, and requires research efforts. Though the proposed algorithm is designed for dehazing, it can also be used for other tasks, e.g. contrast enhancement in other environment. If some work of signal adaptation is done, its application field can be extended more.

References

[1] S. M. Pizer, "Contrast-limited adaptive histogram equalization: Speed and effectiveness stephen m. pizer, r. eugene johnston, james p. ericksen, bonnie c. yankaskas, keith e. muller medical image display research group," in *Proceedings of the First Conference on Visualization in Biomedical Computing, Atlanta, Georgia*, vol. 337, 1990.

[2] K. He, J. Sun, and X. Tang, "Single image haze removal using dark channel prior," *IEEE transactions on pattern analysis and machine intelligence*, vol. 33, no. 12, pp. 2341–2353, 2010.

[3] D. Berman, S. Avidan, *et al.*, "Non-local image dehazing," in *Proceedings of the IEEE conference on computer vision and pattern recognition*, pp. 1674–1682, 2016.

[4] Y. Cho, J. Jeong, and A. Kim, "Model-assisted multiband fusion for single image enhancement and applications to robot vision," *IEEE Robotics and Automation Letters*, vol. 3, no. 4, pp. 2822–2829, 2018.

[5] H. Israël and F. Kasten, "Koschmieders theorie der horizontalen sichtweite," in *Die Sichtweite im Nebel und die Möglichkeiten ihrer künstlichen Beeinflussung*, pp. 7–10, Springer, 1959.

[6] C. I. Gonzalez, P. Melin, J. R. Castro, and O. Castillo, *Edge detection methods based on generalized type-2 fuzzy logic*. Springer, 2017.

[7] K. He, J. Sun, and X. Tang, "Guided image filtering," *IEEE transactions on pattern analysis and machine intelligence*, vol. 35, no. 6, pp. 1397–1409, 2012.

[8] Y.-T. Kim, "Contrast enhancement using brightness preserving bi-histogram equalization," *IEEE transactions on Consumer Electronics*, vol. 43, no. 1, pp. 1–8, 1997.

[9] S.-D. Chen and A. R. Ramli, "Minimum mean brightness error bi-histogram equalization in contrast enhancement," *IEEE transactions on Consumer Electronics*, vol. 49, no. 4, pp. 1310–1319, 2003.

[10] C. H. Ooi and N. A. M. Isa, "Adaptive contrast enhancement methods with brightness preserving," *IEEE Transactions on Consumer Electronics*, vol. 56, no. 4, pp. 2543–2551, 2010.

[11] C. Wang and S. Gong, "Pixel classification algorithms for noise removal and signal preservation in low-pass filtering for contrast enhancement," in *2014 19th International Conference on Digital Signal Processing*, pp. 480–485, IEEE, 2014.

[12] J. A. Stark, "Adaptive image contrast enhancement using generalizations of histogram equalization," *IEEE Transactions on image processing*, vol. 9, no. 5, pp. 889–896, 2000.

[13] Q. Wang and R. K. Ward, "Fast image/video contrast enhancement based on weighted thresholded histogram equalization," *IEEE transactions on Consumer Electronics*, vol. 53, no. 2, pp. 757–764, 2007.

[14] A. Boschetti, N. Adami, R. Leonardi, and M. Okuda, "High dynamic range image tone mapping based on local histogram equalization," in *2010 IEEE International Conference on Multimedia and Expo*, pp. 1130–1135, IEEE, 2010.

[15] Y. Wan and Q. Chen, "Joint image dehazing and contrast enhancement using the hsv color space," in *2015 Visual Communications and Image Processing (VCIP)*, pp. 1–4, IEEE, 2015.

[16] J.-H. Kim, J.-Y. Sim, and C.-S. Kim, "Single image dehazing based on contrast enhancement," in *2011 IEEE International Conference on Acoustics, Speech and Signal Processing (ICASSP)*, pp. 1273–1276, IEEE, 2011.

[17] J.-H. Kim, W.-D. Jang, J.-Y. Sim, and C.-S. Kim, "Optimized contrast enhancement for real-time image and video dehazing," *Journal of Visual Communication and Image Representation*, vol. 24, no. 3, pp. 410–425, 2013.

[18] M. El Ketara and S. Breugnot, "Imaging through haze using multispectral polarization imaging method," in *Polarization: Measurement, Analysis, and Remote Sensing XIII*, vol. 10655, p. 106550N, International Society for Optics and Photonics, 2018.

[19] R. Fattal, "Single image dehazing," *ACM transactions on graphics (TOG)*, vol. 27, no. 3, pp. 1–9, 2008.

[20] R. N. Clark and T. L. Roush, "Reflectance spectroscopy: Quantitative analysis techniques for remote sensing applications," *Journal of Geophysical Research: Solid Earth*, vol. 89, no. B7, pp. 6329–6340, 1984.

[21] S. G. Narasimhan, S. K. Nayar, B. Sun, and S. J. Koppal, "Structured light in scattering media," in *Tenth IEEE International Conference on Computer Vision (ICCV'05) Volume 1*, vol. 1, pp. 420–427, IEEE, 2005.

[22] M. v. van Rossum and T. M. Nieuwenhuizen, "Multiple scattering of classical waves: microscopy, mesoscopy, and diffusion," *Reviews of Modern Physics*, vol. 71, no. 1, p. 313, 1999.

[23] H. Koschmieder, "Theorie der horizontalen sichtweite," *Beitrage zur Physik der freien Atmosphare*, pp. 33–53, 1924.

[24] S. G. Narasimhan and S. K. Nayar, "Vision and the atmosphere," *International journal of computer vision*, vol. 48, no. 3, pp. 233–254, 2002.

[25] S. G. Narasimhan and S. K. Nayar, "Chromatic framework for vision in bad weather," in *Proceedings IEEE Conference on Computer Vision and Pattern Recognition. CVPR 2000 (Cat. No. PR00662)*, vol. 1, pp. 598–605, IEEE, 2000.

[26] R. T. Tan, "Visibility in bad weather from a single image," in *2008 IEEE Conference on Computer Vision and Pattern Recognition*, pp. 1–8, IEEE, 2008.

[27] P. S. Chavez Jr, "An improved dark-object subtraction technique for atmospheric scattering correction of multispectral data," *Remote sensing of environment*, vol. 24, no. 3, pp. 459–479, 1988.

[28] S. K. Nayar and S. G. Narasimhan, "Vision in bad weather," in *Proceedings of the Seventh IEEE International Conference on Computer Vision*, vol. 2, pp. 820–827, IEEE, 1999.

[29] Y. Y. Schechner, S. G. Narasimhan, and S. K. Nayar, "Instant dehazing of images using polarization," in *Proceedings of the 2001 IEEE Computer Society Conference on Computer Vision and Pattern Recognition. CVPR 2001*, vol. 1, pp. I–I, IEEE, 2001.

[30] S. Shwartz and Y. Schechner, "Blind haze separation," in *2006 IEEE Computer Society Conference on Computer Vision and Pattern Recognition (CVPR'06)*, vol. 2, pp. 1984–1991, IEEE, 2006.

[31] P. E. Debevec and J. Malik, "Recovering high dynamic range radiance maps from photographs," in *ACM SIGGRAPH 2008 classes*, pp. 1–10, 2008.

[32] B. Jiang, W. X. Zhang, X. L. Ma, Y. Ru, H. Q. Meng, and L. Wang, "Method for sky region segmentation," *Electronics Letters*, vol. 51, no. 25, pp. 2104–2106, 2015.

[33] A. Sabir, K. Khurshid, and A. Salman, "Segmentation-based image defogging using modified dark channel prior," *EURASIP Journal on Image and Video Processing*, vol. 2020, no. 1, pp. 1–14, 2020.